An Improvement of Realistic Performance of

a Haptic System with an Adaptive Virtual Coupling

Mr. Sompong Lertpolpairoj B. Eng. (Mechanical Engineering)

A Thesis Submitted in Partial Fulfillment of the Requirements

for the Degree of Master of Engineering

Department of Mechanical Engineering

King Mongkut's University of Technology Thonburi

2001

Thesis Committee

..... (Dr. Siam Charoenseang)	Chairman
..... (Dr. Thavida Maneewarn)	Co-Chairman
..... (Assoc. Prof. Dr. Djitt Laowattana)	Member
..... (Assoc. Prof. Dr. Pichit Rerkshanandana)	Member
..... (Dr. Witaya Wannasuphoprasit)	Member

ISBN 974-628-602-1

Copyright reserved

สำนักหอสมุด 22 มิ.ค.

มหาวิทยาลัยเทคโนโลยีพระจอมเกล้าธนบุรี

Thesis Title	An Improvement of Realistic Performance of a Haptic System with an Adaptive Virtual Coupling
Thesis Credits	12
Candidate	Mr. Sompong Lertpolpairoj
Supervisor	Dr. Siam Charoenseang
Degree of Study	Master of Engineering
Department	Mechanical Engineering
Academic Year	2001

Abstract

A high performance haptic system should provide both stable and realistic interaction to users. In order to improve system stability, virtual couplings have been used in order to separate the haptic display from virtual environment simulations. Therefore, it can improve system stability but unfortunately suffers realistic performance. Hence, an interesting problem is to compromise between these two properties.

The contribution of this work is to improve the concept of virtual coupling to meet both stability and realistic performance. This improved concept named adaptive virtual coupling is designed such that its parameters can be adjusted to maximize realistic performance while ensuring stability. The experimental result indicated that users could feel more realistically than by using static virtual coupling (whose parameters are constant).

This thesis presents three results associated with the improved concept. The first result is a new realistic performance index named realistic performance boundaries (RPB). This index can be determined directly from the experiment. By using this concept, the effect of static virtual couplings on realistic performance of haptic systems could be thoroughly examined. The second result is a concept of the adaptive virtual coupling, which is derived by using a simple algorithm. However, this concept could not be implemented directly because the parameters of the virtual coupling are frequency dependent parameters. Therefore, the final result is an algorithm to finding this frequency, which is called an interacting frequency estimator (IFE). Hence the adaptive virtual coupling could be implemented.

Finally, two experiments were set up. The first experiment was aimed at finding the realistic performance boundaries and the second experiment was used as an evaluation on realistic performance of the adaptive virtual coupling.

Keywords : Haptic Interface / Stability of Haptic System Realistic Performance Impedance Display / Passivity / Network Theory

หัวข้อวิทยานิพนธ์	การปรับปรุงประสิทธิภาพด้านความเหมือนจริงของระบบความจริงเสมือนแบบมีแรงป้อนกลับโดยใช้ข้อต่อเสมือนแบบปรับเปลี่ยนค่าได้
หน่วยกิตของวิทยานิพนธ์	12 หน่วย
โดย	นายสมพงศ์ เลิศผลไพโรจน์
อาจารย์ที่ปรึกษา	ดร. สยาม เจริญเสียง
ระดับการศึกษา	วิศวกรรมศาสตรมหาบัณฑิต
ภาควิชา	วิศวกรรมเครื่องกล
ปีการศึกษา	2544

บทคัดย่อ

ระบบแฮปติกส์เป็นระบบซึ่งใช้ในการสร้างแรงป้อนกลับ และการเคลื่อนที่ให้ผู้ใช้ โดยแรงและการเคลื่อนที่ที่ผู้ใช้ได้รับต้องสอดคล้องกับแรงและการเคลื่อนที่ของวัตถุเสมือน ระบบแฮปติกส์ที่มีประสิทธิภาพสูงต้องสามารถสร้างแรงป้อนกลับที่เหมือนจริง กล่าวคือแรงป้อนกลับดังกล่าวต้องสามารถทำให้ผู้ใช้รู้สึกเสมือนตนเองกำลังปฏิสัมพันธ์กับสภาวะแวดล้อมที่มีอยู่จริง และในขณะเดียวกันระบบต้องมีเสถียรภาพในขณะใช้งานด้วย ดังนั้นข้อต่อเสมือนถูกนำมาใช้ในการรักษาเสถียรภาพ โดยข้อต่อนี้เชื่อมต่อระหว่างอุปกรณ์แฮปติกส์ และการจำลองสภาวะแวดล้อมเสมือน แต่ข้อเสียของการนำข้อต่อเสมือนมาใช้คือทำให้ประสิทธิภาพด้านความเหมือนจริงลดลง ดังนั้นวิทยานิพนธ์นี้เป็นการหาวิธีในการถ่วงดุลกันระหว่างประสิทธิภาพด้านความเหมือนจริงและเสถียรภาพของระบบแฮปติกส์

ประโยชน์ที่ได้รับจากงานนี้คือการพัฒนาข้อต่อเสมือนเพื่อให้ระบบแฮปติกส์มีประสิทธิภาพด้านความเหมือนจริงสูงขึ้นกว่าข้อต่อเสมือนแบบเดิม และระบบยังคงมีเสถียรภาพด้วย โดยข้อต่อเสมือนนี้ซึ่งเรียกว่า ข้อต่อเสมือนแบบปรับค่าได้ เป็นข้อต่อเสมือนซึ่งสามารถปรับค่าพารามิเตอร์ของตัวเองเพื่อให้มีประสิทธิภาพด้านความเหมือนจริงสูงสุด เท่าที่ยังคงสามารถรักษาเสถียรภาพได้ จากผลการทดลองชี้ให้เห็นว่าผู้ใช้สามารถรู้สึกถึงแรงป้อนกลับที่เหมือนจริงมากกว่าการใช้ข้อต่อเสมือนแบบเดิม

ประเด็นหลักในวิทยานิพนธ์นี้แบ่งได้เป็นสามส่วน ส่วนแรกเป็นการเสนอดัชนีที่ใช้บ่งบอกประสิทธิภาพด้านความเหมือนจริงตัวใหม่ ชื่อขอบเขตประสิทธิภาพด้านความเหมือนจริง โดยดัชนีนี้สามารถหาได้โดยตรงจากการทดลอง ดังนั้นเราสามารถหาผลกระทบของการใช้ข้อต่อเสมือนแบบเดิมที่มีต่อความเหมือนจริงของระบบแฮปติกส์ ส่วนที่สองเป็นการเสนอการปรับปรุงข้อต่อเสมือน โดยใช้ข้อต่อเสมือนแบบปรับค่าได้ โดยข้อต่อนี้สามารถแก้ปัญหาความไม่เหมือนจริงที่เกิดจากการใช้ข้อต่อเสมือนแบบเดิม แต่การใช้ข้อต่อแบบนี้จำเป็นต้องทราบความถี่ในการปฏิสัมพันธ์ ดังนั้นส่วนสุดท้าย กล่าวถึงการหาความถี่ในการปฏิสัมพันธ์เพื่อใช้ปรับค่าพารามิเตอร์ของข้อต่อเสมือน

คำสำคัญ (Keywords) : ระบบแฮปติกส์ / เสถียรภาพของระบบแฮปติกส์ / ทฤษฎีร่างแห
ประสิทธิภาพด้านความเหมือนจริง / อิมพีแดนซ์ / พาสซีวิตี้

Acknowledgements

I would like to give my best appreciation to my advisors, Dr. Siam Charoenseang and Dr. Thavida Maneewarn. Many ideas were initiated from them. Dr. Siam has helped me to formulate many concepts when this research was infancy, while Dr. Thavida has took part in many deeply details. Special esteem is giving to Assoc. Prof. Dr. Djitt Laowattana, for providing me with a research environment at Center of operation for FIeld roBOtics development (FIBO). Many of my working and thinking methods are shaped by him. I would like to thanks to Assoc. Prof. Dr. Pichit Rerkshanandana for his advice in building hardware at the beginning of this project. Dr. Pichit always has great solutions in all questions. My best acknowledgement is for Dr. Witaya Wannasuphoprasit, who is a specialist in haptic interface, for ensuring that this document is technically sound and relevant. My highly acknowledgement is given to the Thailand Research Fund (TRF) in providing research funding to this project. I would like to thank to all members at FIBO who have helped me in many aspects. Finally, I could never finish my work if there is no any support from my father and mother.

Contents

		Page
English Abstract		ii
Thai Abstract		iv
Acknowledgements		vi
Contents		vii
List of Tables		x
List of Figures		xi
Nomenclatures		xiii
Chapter 1	Introduction	1
	1.1 Background	1
	1.2 State of the Art	3
	1.3 Objectives	4
	1.4 Contributions	5
	1.5 Organization of the Document	6
Chapter 2	Review of Linear Network Theory	7
	2.1 An n-Port Network Representation	7
	2.2 Passivity	10
	2.3 Two-Port Representation and Stability Analysis	12

Chapter 3	Haptic System Modeling and Stability Criteria		15
	3.1	Impedance Display Haptic System Modeling	16
	3.2	Stability of Haptic System	19
	3.3	Virtual Coupling	20
	3.4	High Bandwidth Force Display (HBFD): Modeling and Stability Analysis	22
Chapter 4	Realistic Performance of Haptic Systems		27
	4.1	Realistic Performance Boundaries	28
	4.2	Experimental Procedure	30
Chapter 5	Adaptive Virtual Coupling		33
	5.1	An Algorithm of Determining Parameters of the Adaptive Virtual Coupling	34
	5.2	Implementation Procedure	41
Chapter 6	Experimental Results and Discussion		45
	6.1	Experiment I: Determination of the Realistic Performance Boundaries	46
	6.2	Calculation of the Parameters for the Adaptive Virtual Couplings	52
	6.3	Experiment II : Evaluating the Realistic Performance of Adaptive Virtual Couplings	61

Chapter 7 Conclusions and Further Works 66

Reference 68

List of Tables

Table		Page
3.1	Parameters of the High Bandwidth Force Display (HBFD)	24
6.1	Experimental Results on the Determination of the Realistic Performance Boundaries	47
6.2	Experimental Results on the Matching of the Virtual Environment	62

List of Figures

Figure		Page
2.1	Schematic Diagram of an n-Port Network, N_n	8
2.2	The Symbolic Representation of an n-Port Network in Vector Form	8
2.3	Schematic Diagram of a Linear Two-Port Network	12
3.1	Haptic System Components	15
3.2	Impedance Display Haptic System	16
3.3	Schematic Diagram of a Haptic System with a Virtual Coupling	20
3.4	High Bandwidth Force Display (HBFD)	22
3.5	An Eight-Order Mass, Spring and Damper Model of the High Bandwidth Force Display (HBFD)	23
3.6	Stability Criteria of an Impedance Haptic Display	25
4.1	Realistic Performance Boundaries of a Haptic Interaction	29
5.1	Plot of the Objective Function (J) of an Adaptive Virtual Coupling	37
5.2	Contour of the Objective Function of an Adaptive Virtual Coupling	38
5.3	(a) Contour of the Objective Function when $\mathrm{Re}(Z_{h_avc}(z)) \geq 0$ (b) Contour of the Objective Function when $\mathrm{Re}(Z_{h_avc}(z)) < 0$	39
5.4	Schematic Diagram of a Haptic System with an Adaptive Virtual Coupling	42
5.5	Schematic Diagram Shows that the Haptic System is a LTI System	42
5.6	Spectral Density of the Velocity of a Haptic Interaction	43
6.1	Virtual Wall Simulation	46

6.2	Plot of Realistic Performance Boundaries	49
6.3	Plot of the Results on the Determination of the Adaptive Virtual Coupling of VE2	53
6.4	Plot of the Results on the Determination of the Adaptive Virtual Coupling of VE3	54
6.5	Plot of the Results on the Determination of the Adaptive Virtual Coupling of VE4	55
6.6	Plot of the Results on the Determination of the Adaptive Virtual Coupling of VE5	56
6.7	Plot of the Results on the Determination of the Adaptive Virtual Coupling of VE6	57
6.8	Plot of the Results on the Determination of the Adaptive Virtual Coupling of VE7	58
6.9	A Simulation Used as an Evaluation of Realistic Performance	61
6.10	Plot of the Experimental Results on the Matching of the Virtual Environment	63

Nomenclatures

b	=	Damping
F	=	Force
G	=	Alternative Hybrid Matrix
H	=	Hybrid Matrix
I	=	Current
Im	=	Imaginary Part
J	=	Objective Function
k	=	Stiffness
m	=	Mass
n	=	Number of Sample
P	=	Immittance Matrix
Re	=	Real Part
s	=	Laplace Operator
S_v	=	Spectral Density
T	=	Sampling Period
$t_{\alpha/2,\nu}$	=	t-Distribution Value
u	=	Input Vector
V	=	Voltage
v	=	Velocity
$\overline{X}$	=	Mean
Y	=	Admittance Matrix
y	=	Output Vector

Z	=	Impedance
z	=	z-Transform Operator
ω	=	Frequency

Subscriptions:

avc	=	Adaptive Virtual Coupling
c	=	Virtual Coupling
d	=	Device
ds	=	Desired Impedance
e	=	Virtual Environment
h	=	Human
L	=	Lower Bound
U	=	Upper Bound
vc	=	Static Virtual Coupling

Chapter 1

Introduction

This thesis presents the development of a haptic interface system with an adaptive virtual coupling. This system, aimed at maximizing realistic performance while guaranteeing system stability, is mathematically analyzed. Overall performance of haptic system would be increased. Haptic system, in general, comprises of three components, i.e. human operator, haptic device and virtual environment simulation. Interaction of the operator, which could be sensed in form of force, position or velocity, is used as an input information for the simulation. Virtual environment simulation is derived behavior of virtual environment in form of motion or force depending on input data and control algorithm. Once a simulation is calculated at every sampling time, a haptic device, an electromechanical device, is controlled to produce force feedback corresponding to motion of the virtual environments.

1.1 Background

Nowadays, we are in the world of increased computer usage ranging from personal usage, manufacturing, to entertainment. Therefore, research in communication modalities between human and computers is a very active research area. The objectives of these researches are to promote natural feeling of human

while interacting with computers. Virtual reality, a recent human-computer interaction form, was introduced for this purpose.

Visual-based interaction, a VR interaction modality, while very useful for many applications, is sometimes insufficient to give the user a sense of immersion in the virtual environment. Many simulations, especially ones that involve manual dexterity, require haptic sensation to allow user to understand the digital information. Good examples include a simulation of motor skill training or surgery simulation. Therefore, haptic interface can be integrated into many simulations to provide force feedback to human. In order to let user feels like he/she completely is immersed into the virtual world, force feedback must correspond to visual feedback to fulfill hand-eyes coordination. Not only the correspondence of force and visual interface, but also the safety of the interaction should be seriously concerned. Human interacts with haptic system directly hence it can cause a physical injury if the system is unstable. For these reasons, the main objective of haptic interface is to provide realistic feeling to users while maintaining stability.

Many researches have been explored the aspect of stability in haptic system for ensuring haptic system stability. Colgate and his colleague [1] proposed a linear two-port network named virtual coupling in order to guarantee system stability. Such component is used to couple simulation of a virtual environment and haptic device. The passivity concept developed by Colgate and Schenkel [2] was applied to determine parameters of haptic devices. These parameters are necessary for achieving system stability. Hannaford and Adams [3][4][5][6] also implemented a virtual coupling in their system. When each end of this coupling is connected with passive environment and human, necessary and sufficient conditions of the virtual

coupling which guarantee system stability could be determined. Ryu and Hannaford [7] used a time domain passivity control in order to regulate the excess energy and perform a real-time dissipation. However, while enhancing the system stability, such a virtual coupling affects the realism of haptic simulation due to coupling impedance. The virtual coupling behaves like a mechanical coupling element connecting between a haptic device and virtual environment simulations.

A high performance haptic interface should allow users to feel like he or she interacts with real environment while, in fact, interacting with virtual environment. Hence, the transparency defined as a quality of force and velocity transformation of haptic systems is a very crucial property in the required performance. Colgate and Brown [8] used a dynamic range of achievable impedance so called "Z-Width" to measure the performance of force reflecting interfaces. Furthermore, Lawrence [9] proposed a concept of "Ideal-Equivalent" which considers the limitation of human sensation. By knowing this limitation, an impedance objective, a range of realistic interaction impedance sufficiently convincing users, could be determined. Yokokohji and his colleagues [10] proposed a concept of visual/haptic interfaces called "What You can See Is What You can Feel (WYSIWYF)". This concept benefits from using correct visual/haptic registration in enhancing realism.

1.2 State of the Art

The concept of transparency was mainly discussed in two types of motion: free motion and constraint motion. However, in actual simulation, the impedance during interaction processes usually varies considerably from these two cases above. Moreover, there is not always necessary to maximize transparency because human

perception has limitation. Thus, more transparency not only decreases stability but also does not mean higher realistic performance. Therefore, we propose a new method in performance measuring called "realistic performance boundaries".

The previous analysis illustrates that the use of a static virtual coupling is to ensure global stability of the haptic system, while it does not concern about the realistic performance of the system. However, there still is excess stability margin during some interaction. This means that in some interactions, the virtual coupling is too compliant to just ensure system stability. Thus, the realistic performance would be affected. This effect could be eliminated or lowered by adjusting the parameters of the virtual coupling, depending on interaction, to maximize transparency while ensuring stability. Therefore, we propose a new concept of virtual coupling named adaptive virtual coupling. This coupling can adjust its parameters to the optimized parameters depending on interaction frequency. Therefore, an interacting frequency estimator (IFE) was introduced for the purpose of resolving user interaction frequency, such that the adaptive virtual coupling could be implemented.

1.3 Objectives

The first objective is to propose a new method in performance measurement called "realistic performance boundaries". These boundaries depend on simulation impedance. A haptic system satisfies realistic interaction if the displayed impedance is in these boundaries. We can determine the realistic performance of any virtual environment despite of free-motion or constraint-motion. Therefore, the effect of the

fixed virtual coupling on realistic performance could be thoroughly examined in frequency domain.

The second objective is to enhance the realistic performance of haptic system by proposing an adaptive virtual coupling. This coupling could adjust its parameters according to haptic interaction. An experiment was setup to evaluate the performance of this coupling comparing to static virtual coupling, whose parameters are not function of time.

1.4 Contributions

The first contribution is to propose a new realistic performance index named realistic performance boundaries. This index can be found directly from an experiment. By using these boundaries, we have found that the unrealistic characteristics of haptic simulation depend on several factors. One of them is the virtual coupling. Our preliminary study is to analyze the effect of a static virtual coupling on realistic performance of a haptic system (High Bandwidth Force Display: HBFD built by Moreyra and Hannaford [11][15]) by using realistic performance boundaries. Our study aims at understanding fundamental relationship between stability and transparency such that we can optimize these two properties further. The second contribution is to propose an adaptive virtual coupling to compromise between stability and transparency. Such coupling parameters could be derived with respect to frequency by using a simple algorithm. We also evaluate the performance of an adaptive virtual coupling comparing to a static virtual coupling and no virtual coupling.

1.5 Organization of the Document

Chapter 1 describes some introduction to the field of haptic interface, state of the art, objectives, contributions and organization of the document. Chapter 2 presents several essential materials used in our analysis which are an n-port network representation, passivity concept and two-port representation and its stability criteria. The haptic system modeling and stability criteria are mentioned in Chapter 3. The virtual coupling concept used for improving system stability is introduced herein. At the last of this chapter, our testbed is analyzed both in mathematical modeling and stability. A new concept of realistic performance measurement called realistic performance boundaries is proposed in chapter 4. The experimental procedure for this concept is also presented. Chapter 5 proposes an algorithm for determining parameters of the adaptive virtual coupling. The implementing procedure is also presented in detail. The experimental results of both finding the realistic performance boundaries and implementing adaptive virtual coupling are shown in Chapter 6. The conclusion and discussion are described in the last chapter.

Chapter 2

Review of Linear Network Theory

This chapter reviews some fundamental concepts of the linear network theory. We use this theory for our haptic system modeling and stability analysis through out this document. The reason for choosing this theory as our analysis method is that haptic systems are systems that used for conveying force and velocity between virtual environment and human operator. Thus, there is energy transformation between these two components. The network theory, which basically dealing with electrical circuit analysis, is a method that represents the nature of haptic system, which has energy exchange.

2.1 An n-Port Network Representation

The linear network theory, in Kuh and Rohrer [13], was originated as a tool for analyzing electrical circuit systems. The fundamental concept of this network system is to characterize the input/output signal of an n-terminal pair linear system. Behavior of this system could be determined based on system energy analysis. At the beginning, we consider an n-port network as shown in figure 2.1.

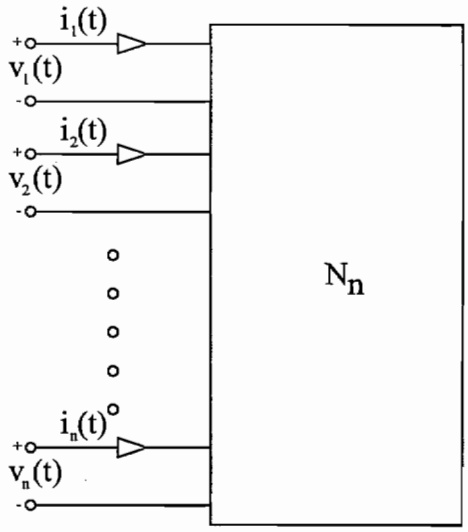

Figure 2.1 Schematic Diagram of an n-Port Network, N_n [13]

This network represents an electrical device to which the only access is by means of a set of n terminal pairs. Each pair is capable of supporting a single real-valued voltage and current. From figure 2.1, the voltage and current of each terminal are represented by $v_1(t), v_2(t), \ldots, v_n(t)$ and $i_1(t), i_2(t), \ldots, i_n(t)$ respectively where t is time and n is number of terminal. This system could be simplified by rewriting in vector form as shown in figure 2.2,

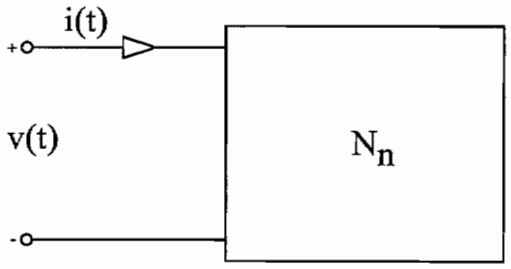

Figure 2.2 The Symbolic Representation of an n-Port Network in Vector Form [13]

where $$V(t) = [v_1(t), v_2(t), \ldots, v_n(t)]^T, \qquad (2.1)$$

and $$I(t) = [i_1(t), i_2(t), ..., i_n(t)]^T . \quad (2.2)$$

The superscripted 'T' represents transpose of the vector. An n-port network can be described by

$$[V(t), I(t)]_{t0}^{tf} \in N_n . \quad (2.3)$$

The relationship between voltage and current of an n-port network can be characterized by a transfer function Z(s) as

$$\{[V(t), I(t)]_{t0}^{tf} : V(s) = Z(s)I(s)\} = N_n , \quad (2.4)$$

where s is a Laplace operator.

As mentioned in the beginning of the chapter that this network theory, which was originally defined for electrical systems, could represent the nature of haptic system because the nature of all systems, in fact, could be analyzed based on energy analysis. Hence, network theory does not restricted to be used only with electrical system but also can be used with another system, which has energetic interaction between elements. Haptic systems are also electromechanical systems, which have energy interaction between human and virtual environment. Thus we can use network theory for analysis. The analogy between electrical system and mechanical system could be described as effort and flow, which characterize each terminal pair of the network. The effort is represented by voltage in electrical system

and by force in mechanical system, while flow is represented by current in electrical system and by velocity in mechanical system.

The next section describes passivity concept, which is a stability concept used with network theory.

2.2 Passivity

In actual implementation, manipulator systems usually interact with environment. Therefore, interaction with environment plays an important role to the analysis of system stability. Passivity concept is an input/output stability concept that is used for determining the stability of such systems by observing the energy generated from the system. An n-port network system described in equation (2.3) is said to be passive if for all admissible signal pair

$$\int_{t_0}^{t} V^T(\tau) I(\tau) d\tau + \varepsilon(t_0) \geq 0, \tag{2.5}$$

for all initial time t_0 and all time $t \in [t_0, \infty]$ where $\varepsilon(t_0)$ is an arbitrary finite energy stored in the network at the initial time t_0 and

$$\int_{t_0}^{t} V^T(\tau) I(\tau) d\tau, \tag{2.6}$$

is the net energy delivered to the n-port network from the external environment via the n accessible ports over the time interval $t \in [t_0, \infty]$.

As shown in equation (2.5), a system is called a passive system if it does not generate the excess energy, in which makes the overall energy exceeds the initial stored energy. For this reason interaction between two or more passive systems always stable.

In order to analyze the network in frequency domain, suppose that $Z(s)$ is a continuous-time linear time invariant transfer function, this system is said to be passive if the transfer function is positive real. Therefore, passivity condition can be written as

$$\mathrm{Re}(Z(j\omega)) \geq 0 \qquad \forall \omega \in R, \tag{2.7}$$

where ω and $Z(j\omega)$ are frequency and impedance matrix respectively while $\mathrm{Re}(\ )$ represents real-part. Moreover, from the derivation of Colgate and Brown [2][16], the passivity concept is not restricted to be used only in continuous-time system but also can be used with the discrete-time system. Suppose that $Z(z)$ is a discrete-time linear time invariant transfer function, this system is passive

$$\mathrm{Re}(Z(z)) \geq 0,\ z = e^{j\omega T} \text{ and } \forall \omega > 0, \tag{2.8}$$

where T is sampling period.

2.3 Two-port Representation and Stability Analysis

Consider a continuous-time/discrete-time linear two-port network as shown in figure 2.3.

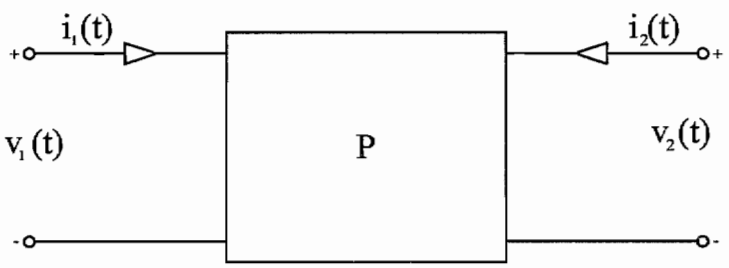

Figure 2.3 Schematic Diagram of a Linear Two-Port Network

The relationship between effort and flow is described by an immittance matrix. An immittance matrix P is a mapping between two vectors, i.e. y and u, where $y = Pu$ and $y^T u = v_1 i_1 + v_2(-i_2)$. Thus, the vector y, u and the immittance matrix P could possible be arranged in four forms as

$$y = Zu, \begin{bmatrix} v_1 \\ v_2 \end{bmatrix} = \begin{bmatrix} z_{11} & z_{12} \\ z_{21} & z_{22} \end{bmatrix} \begin{bmatrix} i_1 \\ -i_2 \end{bmatrix} \tag{2.9}$$

$$y = Yu, \begin{bmatrix} i_1 \\ -i_2 \end{bmatrix} = \begin{bmatrix} y_{11} & y_{12} \\ y_{21} & y_{22} \end{bmatrix} \begin{bmatrix} v_1 \\ v_2 \end{bmatrix} \tag{2.10}$$

$$y = Hu, \begin{bmatrix} v_1 \\ -i_2 \end{bmatrix} = \begin{bmatrix} h_{11} & h_{12} \\ h_{21} & h_{22} \end{bmatrix} \begin{bmatrix} i_1 \\ v_2 \end{bmatrix} \tag{2.11}$$

$$y = Gu, \begin{bmatrix} i_1 \\ v_2 \end{bmatrix} = \begin{bmatrix} g_{11} & g_{12} \\ g_{21} & g_{22} \end{bmatrix} \begin{bmatrix} v_1 \\ -i_2 \end{bmatrix} \tag{2.12}$$

As shown in equation (2.9) to equation (2.12), Z, Y, H and G are called impedance matrix, admittance matrix, hybrid matrix and alternative hybrid matrix, respectively. Although the relation for each mapping is not seem the same but they could be analyzed by using the same method. Suppose that the immittance matrix is represented by P as

$$y = Pu, P = \begin{bmatrix} p_{11} & p_{12} \\ p_{21} & p_{22} \end{bmatrix}. \tag{2.13}$$

The immittance matrix in equation (2.13) could be both continuous-time P(s) and discrete-time P(z) forms. Therefore, the stability of a two-port network depends on its terminal immittance. From equation (2.13), the continuous-time network is passive if and only if the immittance mapping satisfies

$$\mathrm{Re}(P(j\omega)) \geq 0, \ \forall \omega \in R. \tag{2.14}$$

The discrete-time network is passive if and only if the immittance mapping satisfies

$$\mathrm{Re}(P(z)) \geq 0, \ z = e^{j\omega T} \text{ and } \forall \omega > 0. \tag{2.15}$$

Equation (2.15) can be rewritten as

$$\mathrm{Re}(p_{11}) \geq 0,\ \mathrm{Re}(p_{22}) \geq 0, \tag{2.16}$$

$$\mathrm{Re}(p_{11})\mathrm{Re}(p_{22}) - \left|\frac{p_{21}+p_{12}}{2}\right|^2 \geq 0, \forall \omega > 0. \tag{2.17}$$

Our derivation on stability of network is based on the fact that a passive network will always stable when interacting with passive operators. This concept is very conservative because it allows for arbitrary passive two-port terminations. However, there is a less conservative stability concept called unconditional stability. A linear two-port system is unconditionally stable if and only if there is no set of passive termination one-port immittances for which the system is unstable. For a linear time invariant two-port network, Llewellyn's stability criteria provides both necessary and sufficient conditions for unconditionaly stability if

$$\mathrm{Re}(p_{11}) \geq 0,\ \mathrm{Re}(p_{22}) \geq 0, \tag{2.18}$$

$$2\mathrm{Re}(p_{11})\mathrm{Re}(p_{22}) \geq |p_{12}p_{21}| + \mathrm{Re}(p_{12}p_{21}), \forall \omega > 0 \tag{2.19}$$

This stability concept is very important for determining parameters of the virtual coupling, a synthesis coupling used for ensuring system stability, which will be discussed in the next chapter.

Chapter 3

Haptic System Modeling and Stability Criteria

This chapter addresses the mathematical modeling and stability criteria of haptic systems. A haptic system, in general, is comprised of three components, which are human operator, haptic device and virtual environment simulation as shown in figure 3.1.

Figure 3.1 Haptic System Components

The main purpose of haptic system is to produce a stable and a realistic force interaction to users. Therefore, the stability and the realistic performance of haptic systems should be concerned. The haptic system allows user to haptically interact with any preprogrammed virtual environment, such that there is energy transformation between these two components. Thus, network theory can be used as our tool for modeling and analyzing the system stability. The first section describes the modeling of an impedance display haptic system. The stability analysis of haptic system is mentioned in the second section, while the virtual coupling concept is

presented in the third section. Finally, our testbed, High Bandwidth Force Display (HBFD), is analyzed in the last section.

3.1 Impedance Display Haptic System Modeling

There are two paradigms of force feedback generation, i.e. impedance display and admittance display. A haptic system, which measures motion (position and/or velocity) and produces force feedback corresponding to the motion, is called an impedance display haptic system. A haptic system is called admittance display if the feedback motion is calculated from the measured force. In order to simplify the problem, this research deals with only a linear one-degree of freedom impedance display haptic system as shown in figure 3.2.

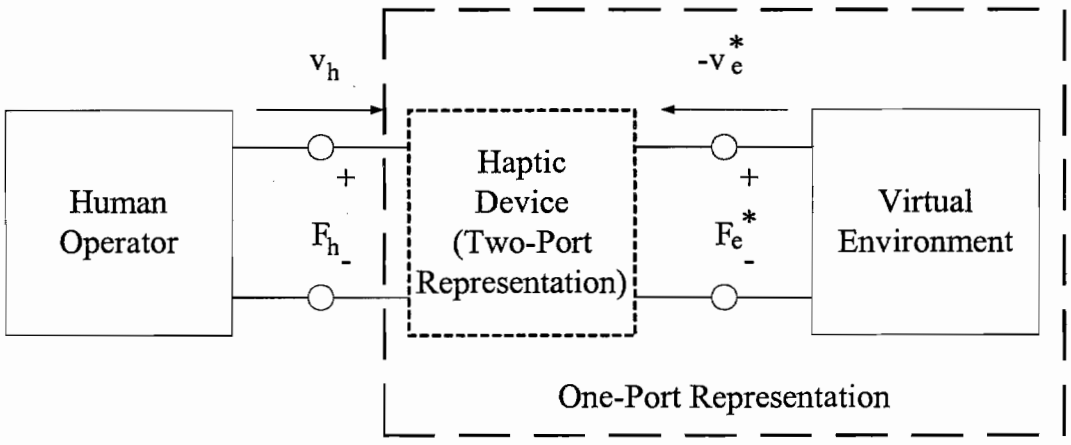

Figure 3.2 Impedance Display Haptic System

From the experiment of Hogan [13], the human operator can be assumed as a Linear Time Invarient system. Therefore, all components, i.e. human operator, haptic device and virtual environment, are assumed to be Linear Time Invariant

(LTI) systems. From figure 3.2, F_h, v_h, F_e and v_e represent human force, human velocity, virtual environment force and virtual environment velocity, respectively. The parameters with "*" are in discrete form. The mathematical model of this system could be derived in one-port and two-port representations.

The one-port representation is described in form of human perceived impedance of haptic system ($Z_h(z)$), which is impedance that human can perceive while interacting with haptic interface.

$$Z_h(z) = Z_d(z) + ZOH(z)Z_e(z) \tag{3.1}$$

From equation (3.1), $Z_d(z)$, $Z_e(z)$ and $ZOH(z)$ are impedance of haptic device, impedance of virtual environment and zero-order-hold, respectively. The device impedance, $Z_d(z)$ discretized by the Tustin's method is defined by

$$Z_d(z) = (m_d s + b_d)\Big|_{s \to \frac{2(z-1)}{T(z+1)}}, \tag{3.2}$$

where m_d and b_d are mass and coefficient of viscosity of the haptic device. The virtual environment discretized by Tustin's method is formulated as

$$Z_e(z) = (m_e s + b_e + \frac{k_e}{s})\Big|_{s \to \frac{2(z-1)}{T(z+1)}}, \tag{3.3}$$

where m_e, b_e and k_e are mass, coefficient of viscosity and stiffness of the virtual environment respectively. The zero-order hold operator is considered as a low pass filter:

$$ZOH(z) = \frac{1}{2}\frac{(z+1)}{z}. \tag{3.4}$$

Thus, the human interacting force, which is formulated in one-port representation, is

$$F_h(z) = Z_h(z)V_h(z). \tag{3.5}$$

The haptic system could also be modeled in form of Two-port representation as

$$\begin{bmatrix} F_h \\ -v_e^* \end{bmatrix} = \begin{bmatrix} Z_d(z) & ZOH(z) \\ -1 & 0 \end{bmatrix} \begin{bmatrix} v_h \\ F_e^* \end{bmatrix}. \tag{3.6}$$

The next section will analyze the stability of haptic system both in one-port representation and two-port representation.

3.2 Stability of Haptic System

The stability criteria of haptic system could be derived in both one-port and two-port representations. From equation (2.8), a haptic system, which is modeled by one-port representation, is stable if

$$\mathrm{Re}(Z_h(z)) \geq 0, \forall \omega > 0. \tag{3.7}$$

In order to find the unconditionally stability criteria of a two-port network haptic system, the human operator and the virtual environment should be assumed to be passive operators. By using Llewellyn's stability criteria described in equation (2.18) and equation (2.19), this system would be unconditional stable system if

$$\mathrm{Re}(Z_d(z)) \geq 0,\ \mathrm{Re}(\mathrm{ZOH}(z)) \geq 0, \tag{3.8}$$

$$\frac{\mathrm{Re}(\mathrm{ZOH}(z))}{|\mathrm{ZOH}(z)|} \geq 1, \forall \omega > 0 \tag{3.9}$$

Equation (3.8) is always satisfy because both $\mathrm{Re}(Z_d(z))$, which is damping of haptic device, and $\mathrm{Re}(\mathrm{ZOH}(z))$ are always greater than zero. Equation (3.9) does not satisfy, thus this system is not unconditionally stable. However, it does not mean that the system will always unstable. Therefore, Colgate and his colleague [2] proposed a virtual coupling which is a synthesis coupling. This coupling, which will be described in the next section, is used as a complementary component in order to make the system satisfy unconditionally stability criteria.

3.3 Virtual Coupling

A virtual coupling, a synthesis coupling which is shown in figure 3.3, is used for connecting between the haptic device and the virtual environment in order to improve the stability of haptic interface system.

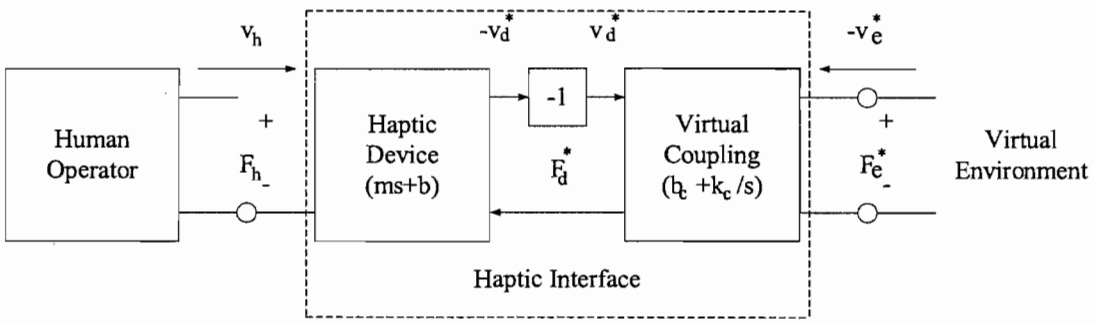

Figure 3.3 Schematic Diagram of a Haptic System with a Virtual Coupling

This coupling could be modeled as any arbitrary structure. As shown in figure 3.3, a spring/damper model is used as our coupling. The impedance of the virtual coupling is

$$Z_c(z) = \left(b_c + \frac{k_c}{s} \right)\Bigg|_{s \to \frac{z-1}{Tz}} \tag{3.10}$$

By changing the impedance from $Z_h(z)$ to $Z_{h_vc}(z)$, the one-port representation of haptic system with virtual coupling can be described as

$$F_{h_vc}(z) = Z_{h_vc}(z)V_h(z), \tag{3.11}$$

where $$Z_{h_vc}(z) = Z_d(z) + ZOH(z)Z_{ec}(z), \tag{3.12}$$

and $$Z_{ec}(z) = \frac{Z_e(z)Z_c(z)}{Z_e(z) + Z_c(z)}. \tag{3.13}$$

The two-port representation of the haptic system with a virtual coupling can be determined from equation (3.6) as

$$\begin{bmatrix} F_h \\ -v_e^* \end{bmatrix} = \begin{bmatrix} Z_d(z) & ZOH(z) \\ -1 & 1/Z_c(z) \end{bmatrix} \begin{bmatrix} v_h \\ F_e^* \end{bmatrix} \tag{3.14}$$

Based on passivity concept in equation (2.8), the haptic system with a virtual coupling is stable if

$$\mathrm{Re}(Z_{h_vc}(z)) \geq 0, \forall \omega > 0. \tag{3.15}$$

From equation (2.18) and equation (2.19), this haptic system with a virtual coupling would be an unconditionally stable system if

$$\mathrm{Re}(Z_d(z)) \geq 0, \ \mathrm{Re}(1/Z_c(z)) \geq 0, \tag{3.16}$$

$$\mathrm{Re}(1/Z_c(z)) \geq \frac{1 - \mathrm{COS}\angle ZOH(z)}{2\,\mathrm{Re}(Z_d(z))} |ZOH(z)| \tag{3.17}$$

From equation (3.17), the virtual coupling could be designed to satisfy the unconditionally stability criteria.

From the impedance point of view, the coupling behaves like a low pass filter between the haptic device and the virtual environment. Thus, in case of a very stiff virtual environment, the haptic device will display the impedance of the virtual coupling instead of the virtual environment. Therefore, the system would stable. The last section briefs about the modeling and stability analysis of our testbed.

3.4 High Bandwidth Force Display (HBFD): Modeling and Stability Analysis

The high bandwidth force display is a two-degrees of freedom Cartesian haptic device built at the University of Washington, Seattle as shown in figure 3.4.

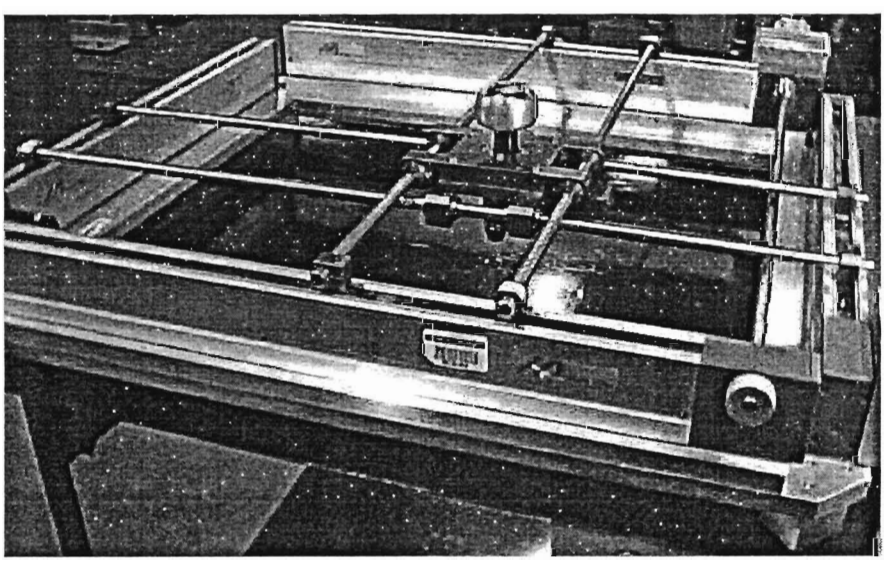

Figure 3.4 High Bandwidth Force Display (HBFD)

This device can produce a high force output of 100 N (peak at 400 N). A fast update rate of 1000 Hz causes this device suitable for haptic simulation. The details of this system can be found in [10]. Each axis can be modeled as an eight-order mass, spring and damper systems as shown in figure 3.5.

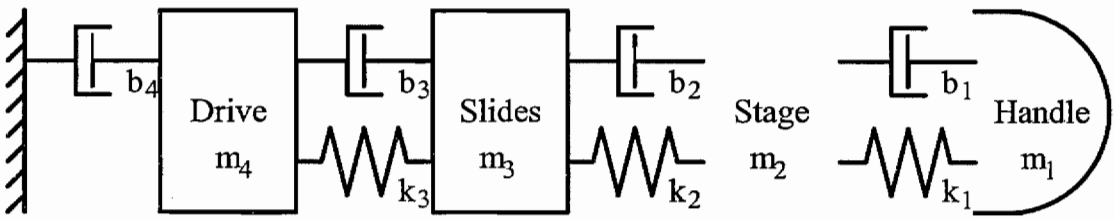

Figure 3.5 An Eight-Order Mass, Spring and Damper Model of the High Bandwidth Force Display (HBFD)

From figure 3.5, four components that should be concerned which are a drive (inertia of torque shaft, motor rotor, couplings, pulleys, cables and bearing), a slider (linear motion bearings and linear motion shaft hangers), a stage (linear bearings and linear motion shaft) and a handle. The impedance of each component is defined as

$$\text{Drive:} \quad Z_{d4}(z) = (m_4 s + b_4)\Big|_{s \to \frac{2(z-1)}{T(z+1)}} \tag{3.18}$$

$$\text{Slider:} \quad Z_{d3}(z) = (m_3 s + b_3 + \frac{k_3}{s})\Big|_{s \to \frac{2(z-1)}{T(z+1)}} \tag{3.19}$$

$$\text{Stage:} \quad Z_{d2}(z) = (m_2 s + b_2 + \frac{k_2}{s})\Big|_{s \to \frac{2(z-1)}{T(z+1)}} \tag{3.20}$$

$$\text{Handle:} \quad Z_{d1}(z) = (m_1 s + b_1 + \frac{k_1}{s})\Big|_{s \to \frac{2(z-1)}{T(z+1)}} \tag{3.21}$$

By summarizing these impedance equations in series form, the impedance of this haptic system is

$$Z_d(z) = \frac{1}{\frac{1}{Z_{d1}(z)} + \frac{1}{Z_{d2}(z)} + \frac{1}{Z_{d3}(z)} + \frac{1}{Z_{d4}(z)}} \tag{3.22}$$

The parameters of these components are shown in table 3.1.

Table 3.1 Parameters of the High Bandwidth Force Display (HBFD)

Components	m (kg)	b (Ns/m)	k (N/m)
Drive	0.5	5	0
Slider	2	118.25	87400
Stage	2.3	60	84000
Handle	0.2	30.93	130000

From this mathematical model of the high bandwidth force display, we can plot the right-hand side of equation (3.17) versus frequency to formulate a theoretical lower bound of $\mathrm{Re}(1/Z_c(z))$. It is plotted as a solid-line in figure 3.5.

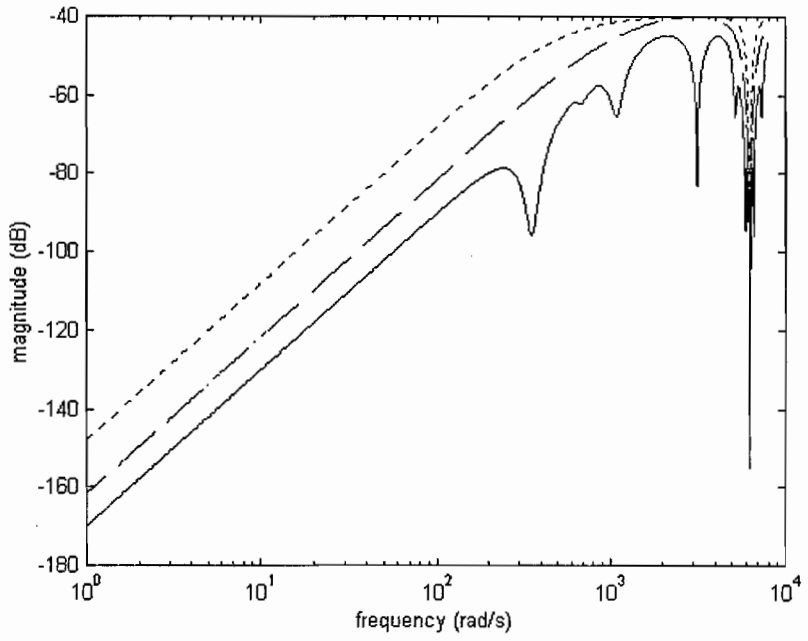

Figure 3.6 Stability Criteria of an Impedance Haptic Display

From the derivation of Hannaford and Adam [6], the theoretical parameters of virtual coupling are as follow: k_c=110 kN/m and b_c=100 Ns/m, plotted in a long-dash-line in figure 3.6. When these parameters are implemented, the system could be easily unstable. This instability results from the fact that the theoretical parameters are the worst case values of virtual coupling. In addition, factors such as nonlinear friction, human operator model and etc. are ignored. By fine tuning the virtual coupling parameters, we have found that the suitable parameters are as follow: k_c=50 kN/m and b_c=100 Ns/m. This new virtual coupling is also plotted as a short-dash-line in figure 3.6.

In this chapter, the stability of haptic interface system is addressed. However, in order to design a high performance haptic system, the realistic performance would be analyzed in the next chapter. Moreover, a new method is

proposed for measuring realistic performance called realistic performance boundaries. This performance index will be used as our parameters for compromising between stability and realism of haptic system.

Chapter 4

Realistic Performance of Haptic Systems

From the previous chapters, the analysis and formulation of virtual coupling that we use can only ensure system stability. However, the realistic performance of haptic system is an essential property too. Realistic performance of a haptic interface can be described in term of "Transparency" which indicates the quality of force and velocity transformation between human and virtual environment. The quality of force and velocity transformation is described in form of human perceived impedance, which was described in equation 3.1 and equation 3.11. There are two cases of human perceived impedance i.e. human perceived impedance of a haptic interface with virtual coupling ($Z_{h_vc}(z)$) and without virtual coupling ($Z_h(z)$). The human perceived impedance of a haptic interface with a virtual coupling ($Z_{h_vc}(z)$) is derived as

$$Z_{h_vc}(z) = Z_d(z) + ZOH(z)Z_{ec}(z), \tag{4.1}$$

where

$$Z_{ec}(z) = \frac{Z_e(z)Z_c(z)}{Z_e(z) + Z_c(z)}. \tag{4.2}$$

The human perceived impedance of the haptic interface without virtual coupling ($Z_h(z)$) is

$$Z_h(z) = Z_d(z) + ZOH(z)Z_e(z). \quad (4.3)$$

The haptic device having a perfect transparency allows the force and velocity perceived by human to be equal to force and velocity of the virtual environment ($F_h = F_e$, $v_h = v_e$). Lawrence [8] proposed a transparency concept called "Ideal-equivalent". This concept is based on the limitation of human perception, related to impedance objectives. These impedance objectives are impedance boundaries which adequately convince the users. These impedance objectives are concerned based on two types of motions, i.e. free motion and constraint motion. The ideal-equivalent concept represents the bound of free and constraint motion, regardless of the realistic performance of the motion which lies between. In fact, types of motion in the real simulation are not restricted in these two cases. For this reason, we propose the realistic performance boundaries, to be thoroughly explained in the next section.

4.1 Realistic Performance Boundaries

The realistic performance boundaries, proposed by Lertpolpairoj and his colleagues [17], represent variation of human perceived impedance ($Z_h(z)$) while stably interacting with the reference environment through a haptic interface without virtual coupling. These boundaries depend on impedance of an adjustable virtual environment. They could be delineated from an experimental data. The parameters of the adjustable virtual environment are adjusted by users. Such that they can perceive this environment to be the same as the reference environment. The adjusted

parameters are analyzed using confidence interval theory to find the range of parameters that satisfies this realistic interaction. The upper and lower values of this range are substituted into the human perceived impedance equation (4.3) and the plot of realistic performance boundaries can be obtained as shown in figure 4.1.

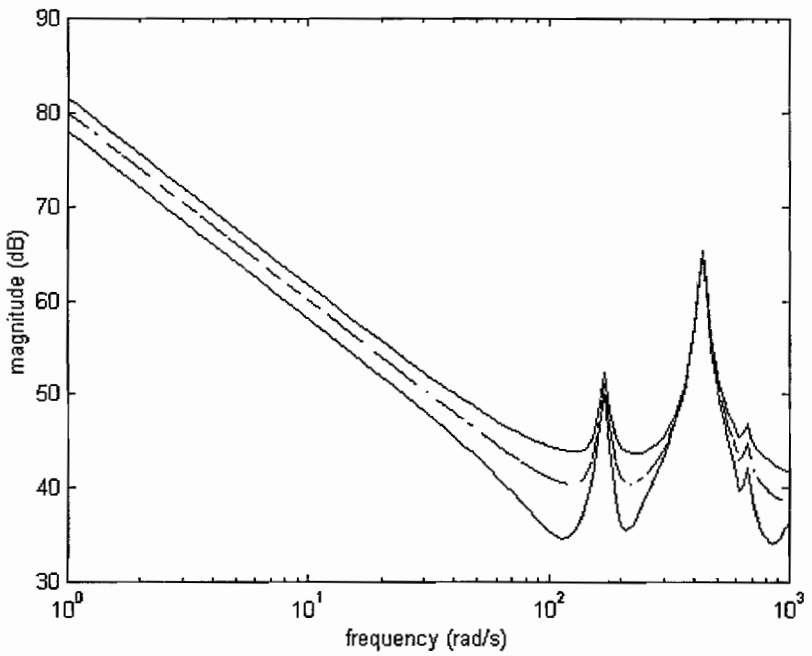

Figure 4.1 Realistic Performance Boundaries of a Haptic Interaction

The dash-line represents the human perceived impedance while interacting with a reference virtual environment. Two solid-lines above and under the dash-line are the upper boundary and lower boundary of the realistic performance boundaries respectively. The band of realistic performance boundaries is defined as the difference between the upper and lower boundaries. The accuracy of these boundaries relies on number of subjects participating in this experiment. If the experimental data is a normal-distribution one, thirty subjects are sufficient to

represent all population (the t-distribution will approach normal-distribution when samples are equal or more than thirty). If we use 99 percent confidence interval, we can conclude that 99 percent of users would feel realistically when the displayed impedance is within this boundary.

4.2 Experimental Procedure

The experimental procedure is carried out step-by-step as follow:

Step 1: Defining a reference virtual environment impedance ($Z_e(z)$) that we want to determine the realistic performance boundaries,

Step 2: Simulating this reference environment on a haptic system (without virtual coupling). Users have to use these interacting forces generated from ($Z_e(z)$) as a reference,

Step 3: Using the same device to simulate another environment called an adjustable virtual environment which has different impedance from the reference virtual environment. Users are required to adjust parameters of this environment until he or she feels as if interacting with the reference environment. Meanwhile, stiffness and damping of this adjusted virtual environment (k_{e_adj} and b_{e_adj}) are observed,

Step 4: Calculating the mean ($\overline{X}$) and the standard deviation (SD) of k_{e_adj} and b_{e_adj} among n users. Using the confidence interval (CI) theory to

determine the range of stiffness and damping that have 99 percent confidence interval.

The $\overline{X}$ and SD are determined as follow:

$$\overline{X} = \frac{\sum_{i=1}^{n} x}{n}, SD = \sqrt{\frac{\sum_{i=1}^{n} (x - \overline{X})^2}{\nu}}, \ \nu = n - 1. \tag{4.4}$$

The upper bound (x_{UCI}) and lower bound (x_{LCI}) of the 99 percent confidence interval of data (x) can be found by

$$x_{LCI} \le x_{confidence} \le x_{UCI}, \text{ and}$$

$$\overline{X} - t_{\alpha/2,\nu}\left(\frac{SD}{\sqrt{n}}\right) \le x_{confidence} \le \overline{X} + t_{\alpha/2,\nu}\left(\frac{SD}{\sqrt{n}}\right) \tag{4.5}$$

where n is number of sample, $x_{confidence}$ is confidence interval, $t_{\alpha/2,\nu}$ is the t-distribution value which have 99 percent confidence interval and $\alpha = 1 - (0.01 \times CI)$.

Step 5: Simply substituting the minimum and maximum of the range of stiffness and damping into the virtual environment model.

We obtain the lower boundary as

$$Z_L(z) = (m_e s + b_{e_LCI} + \frac{k_{e_LCI}}{s})\Big|_{s \to \frac{2(z-1)}{T(z+1)}}, \qquad (4.6)$$

and the upper boundary as

$$Z_U(z) = (m_e s + b_{e_UCI} + \frac{k_{e_UCI}}{s})\Big|_{s \to \frac{2(z-1)}{T(z+1)}}. \qquad (4.7)$$

The realistic performance boundaries are determined by substituting equation (4.6) and equation (4.7) into equation (4.3). A plot of $Z_h(z)$ in equation (4.3) versus frequencies is readily obtained. The result of determining the realistic performance boundaries is summarized in Chapter 6.

From the previous analysis, we obtain two types of performance indexes, which are stability constraint and realistic performance boundaries. The next step is to find a way to compromise between these two performances. Therefore, the adaptive virtual coupling is proposed in Chapter 5.

Chapter 5

Adaptive Virtual Coupling

From Chapter 4, we realize that even though the use of the pre-calculated virtual coupling can ensure system stability when the human operator and the virtual environment are passive, but at the same time the realistic performance is affected. The concept of virtual coupling was derived from the concept of unconditionally stability so that the virtual coupling is static (does not vary with time). Therefore, the stability is always guaranteed for wide range of virtual environment. However, in some cases of interaction this system does not satisfy realistic performance as discussed in the previous chapter. Thus, the objective of this research is to find a method that can be provide the compromising solution between stability and realistic performance of haptic system. This chapter focuses on an improvement in realistic performance of a haptic system by adapting the virtual coupling parameters. However, these parameters must always satisfy stability concept. The virtual couplings, which their parameters are adapted with respect to frequency to satisfy stability condition and realistic performance, are named adaptive virtual couplings.

The first section derives the method of finding these parameters while the second section addresses the implementation of such a coupling.

5.1 An Algorithm for Determining Parameters of an Adaptive Virtual Coupling

The previous chapter gave us the realistic performance boundaries, which are used as our performance index. A haptic system, which can display impedance within these boundaries, can be called a realistic haptic system. This performance index, which is frequency dependent, can be determined for using with any virtual environment by using one-port representation. Thus, one-port representation is used as our derivation on human perceived impedance of haptic system with an adaptive virtual coupling ($Z_{h_avc}(z)$). Assume that $m_e = 0$, thus the mathematical model of $Z_{h_avc}(z)$ can be described as

$$Z_{h_avc}(z) = Z_d(z) + ZOH(z)Z_{e_avc}(z), \tag{5.1}$$

,where

$$Z_{e_avc}(z) = \frac{Z_e(z)Z_{avc}(z)}{Z_e(z) + Z_{avc}(z)} \tag{5.2}$$

and

$$Z_{avc} = \left(b_{avc} + \frac{k_{avc}}{s} \right)\Bigg|_{s \to \frac{(z-1)}{Tz}} \tag{5.3}$$

Suppose that we want to find an adaptive virtual coupling of a virtual environment. The first set of parameters that should be determined are the parameters of the realistic performance boundaries such as the damping and stiffness of the upper bound (b_{e_UCI} and k_{e_UCI}) and the damping and stiffness of the lower

bound (b_{e_LCI} and k_{e_LCI}). After that, the first step is to formulate a desired human perceived impedance ($Z_{h_ds}(z)$), which represents these boundaries as shown in equation (5.4).

$$Z_{h_ds}(z) = Z_d(z) + ZOH(z)Z_{ds}(z), \tag{5.4}$$

, where the desired impedance is

$$Z_{ds} = \left(\frac{(b_{e_UCI} + b_{e_LCI})}{2} + \frac{(k_{e_UCI} + k_{e_LCI})}{2s} \right) \Bigg|_{s \to \frac{T(z-1)}{2(z+1)}}. \tag{5.5}$$

The desired impedance is defined as the impedance, which its magnitude is equally laying between the upper bound and the lower bound. Thus, the parameters of Z_{ds} are the average parameters between the parameters of these two bounds. Reminding that the goal of the adaptive virtual coupling is to maximize the realistic performance while ensuring system stability. Hence, this goal can be mathematically formulated as:

To minimize: $$\left(|Z_{h_ds}(z)| - |Z_{h_avc}(z)| \right)^2, \tag{5.6}$$

Subject to constraint: $$\mathrm{Re}(Z_{h_avc}(z)) \geq 0, \ \forall \omega \in R. \tag{5.7}$$

However, it is not easy to use b_{avc} and k_{avc} as the optimized variables because the impedance equations, i.e. human perceived impedance of haptic system with adaptive virtual coupling ($Z_{h_avc}(z)$) and $Z_{h_ds}(z)$, are all complex functions. Moreover, our constraint, which is described in form of $\mathrm{Re}(Z_{h_avc}(z))$, cannot be easily represented in b_{avc} and k_{avc}. The feasible region of the solution (feasible b_{avc} and k_{avc} that satisfy the objective function and the constraint) is possibly a complicated contour and difficult to be determined. Therefore, in order to simplify our problem we use real part of $Z_{h_avc}(z)$ ($\mathrm{Re}(Z_{h_avc}(z))$) and imaginary-part of $Z_{h_avc}(z)$ ($\mathrm{Im}(Z_{h_avc}(z))$) instead of b_{avc} and k_{avc}. The objective function in equation (5.6) is changed to

$$J = \frac{1}{2}\left[\left(\frac{\mathrm{Re}(Z_{h_ds}(z)) - \mathrm{Re}(Z_{h_avc}(z))}{\mathrm{Re}(Z_{h_ds}(z)) - \mathrm{Re}(Z_{h_avc_max}(z))}\right)^2 + \left(\frac{\mathrm{Im}(Z_{h_ds}(z)) - \mathrm{Im}(Z_{h_avc}(z))}{\mathrm{Im}(Z_{h_ds}(z)) - \mathrm{Im}(Z_{h_avc_max}(z))}\right)^2\right] \qquad (5.8)$$

where the constraint is the same as constraint equation (5.7). The terms $\mathrm{Re}(Z_{h_avc_max}(z))$ and $\mathrm{Im}(Z_{h_avc_max}(z))$ are the maximum real part and imaginary part of the searching space, respectively. Meanwhile, two conditions, i.e. $\mathrm{Re}(Z_{h_avc_max}(z)) \geq \mathrm{Re}(Z_{h_ds}(z))$ and $\mathrm{Im}(Z_{h_avc_max}(z)) \geq \mathrm{Im}(Z_{h_ds}(z))$ must be satisfied in order to ensure that the minimum point is located in the

searching area. Instead of finding the minimum difference between $|Z_{h_ds}(z)|$ and $|Z_{h_avc}(z)|$, the new objective is to find the minimum difference between $\mathrm{Re}(Z_{h_ds}(z))$ and $\mathrm{Re}(Z_{h_avc}(z))$, and between $\mathrm{Im}(Z_{h_ds}(z))$ and $\mathrm{Im}(Z_{h_avc}(z))$. This objective function, plotted in figure 5.1, is a quadratic function which has only one minimum point at

$$[\mathrm{Re}(Z_{h_avc}(z)), \mathrm{Im}(Z_{h_avc}(z))] = [\mathrm{Re}(Z_{h_ds}(z)), \mathrm{Im}(Z_{h_ds}(z))] . \quad (5.9)$$

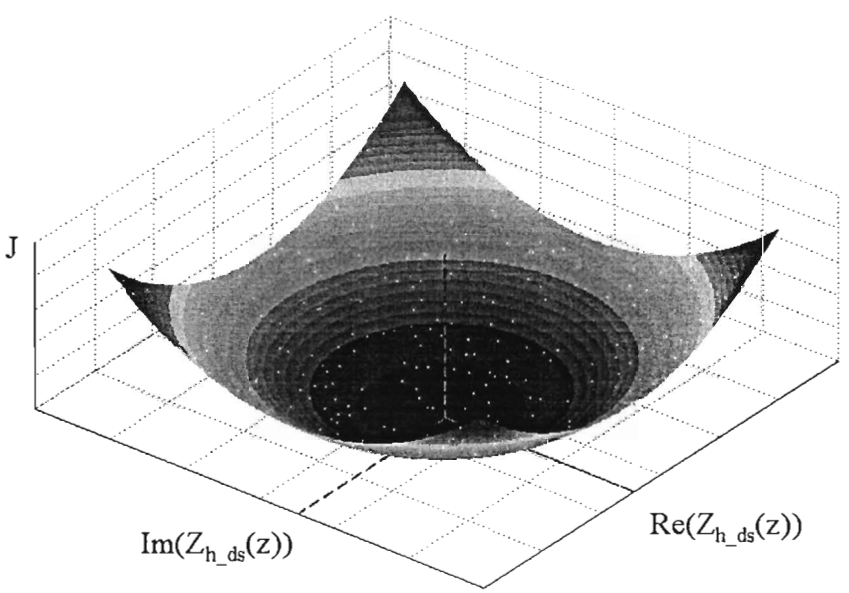

Figure 5.1 Plot of the Objective Function (J) of an Adaptive Virtual Coupling

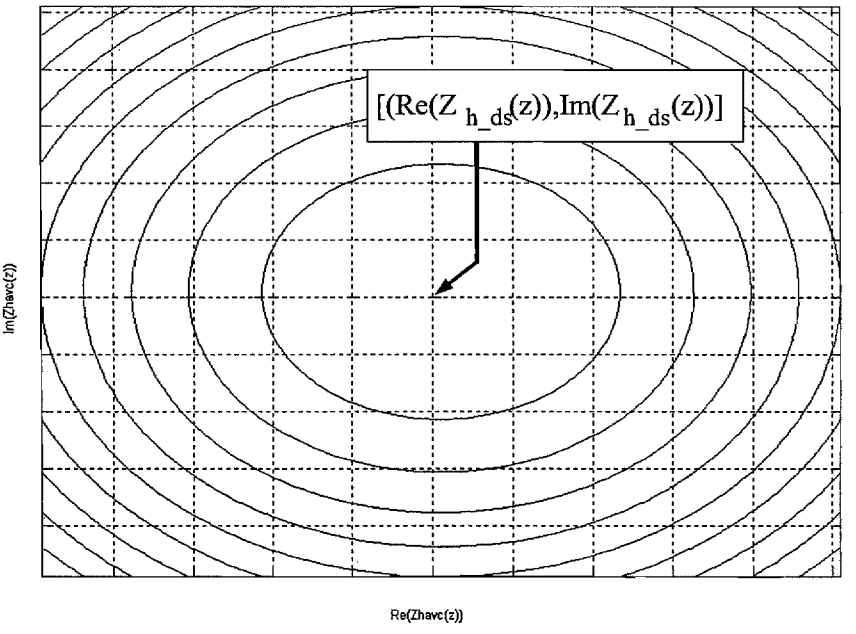

Figure 5.2 Contour of the Objective Function of an Adaptive Virtual Coupling

Figure 5.2 shows the contour of the objective function of an adaptive virtual coupling. The center of this contour is the minimum point of this objective function. From equation (5.7), the constraint is an inequality linear constraint, thus the feasible region can be directly drawn on the contour of the objective function. Such that, there are only two possible cases which are $\mathrm{Re}(Z_{h_avc}(z)) \geq 0$ and $\mathrm{Re}(Z_{h_avc}(z)) < 0$ as shown in figure 5.3.

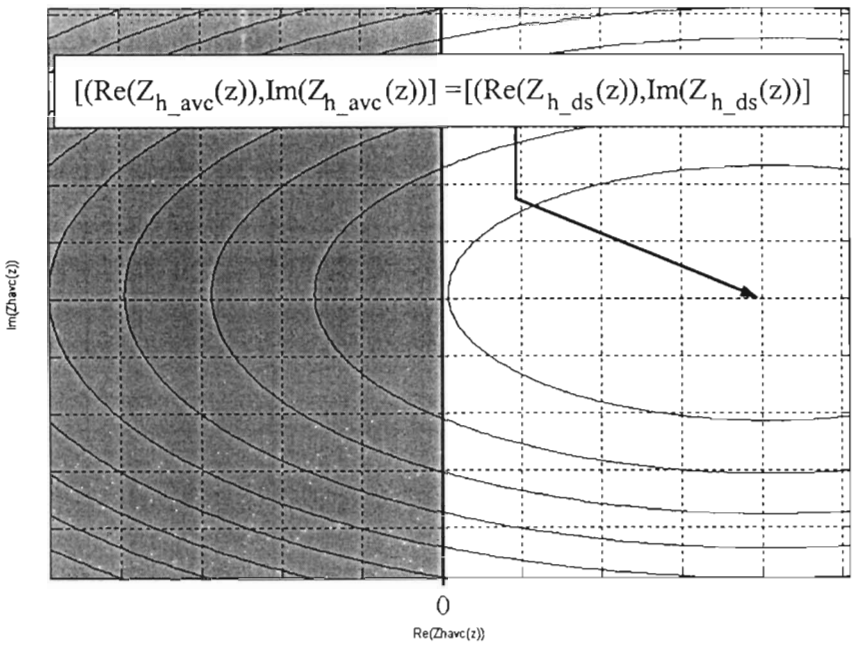

(a)

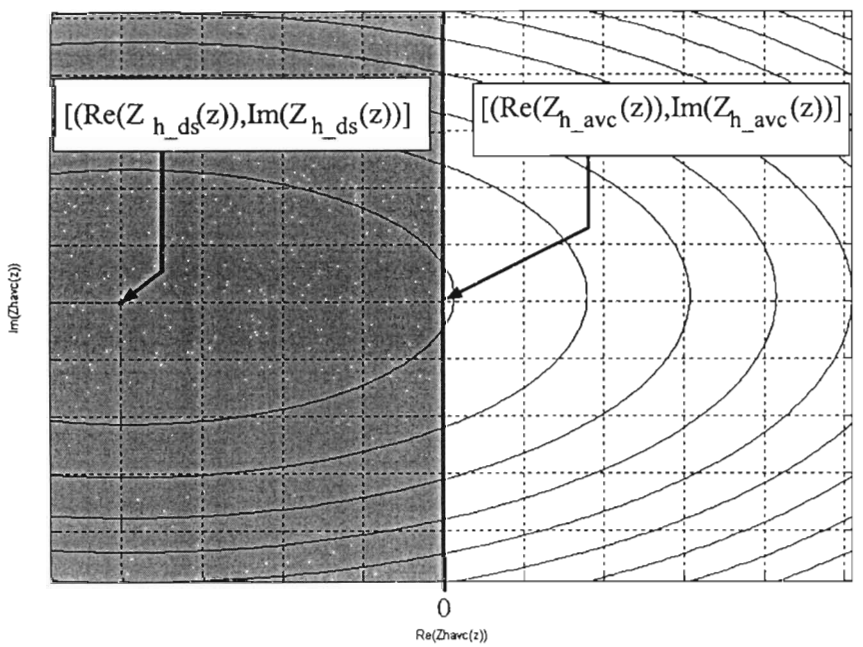

(b)

Figure 5.3 (a) Contour of the Objective Function when $\mathrm{Re}(Z_{h_avc}(z)) \geq 0$

(b) Contour of the Objective Function when $\mathrm{Re}(Z_{h_avc}(z)) < 0$

Therefore, the solutions could be intuitively determined in two cases.

Case 1: $\mathrm{Re}(Z_{h_avc}(z)) \geq 0$

The minimum point which is the solution is

$$[\mathrm{Re}(Z_{h_avc}(z)), \mathrm{Im}(Z_{h_avc}(z))] = [\mathrm{Re}(Z_{h_ds}(z)), \mathrm{Im}(Z_{h_ds}(z))] \quad (5.10)$$

Case 2: $\mathrm{Re}(Z_{h_avc}(z)) < 0$

The minimum point which is the solution is

$$[\mathrm{Re}(Z_{h_avc}(z)), \mathrm{Im}(Z_{h_avc}(z))] = [0, \mathrm{Im}(Z_{h_ds}(z))] \quad (5.11)$$

After $\mathrm{Re}(Z_{h_avc}(z))$ and $\mathrm{Im}(Z_{h_avc}(z))$ are determined, b_{avc} and k_{avc} which are the actual variables that we want to determine can be easily derived by follow these steps.

Step 1: $Z_{h_avc}(z) = \mathrm{Re}(Z_{h_avc}(z)) + j\,\mathrm{Im}(Z_{h_avc}(z))$ (5.12)

Step 2: $Z_{e_avc}(z) = \dfrac{Z_{h_avc}(z) - Z_d(z)}{\mathrm{ZOH}(z)}$ (5.13)

Step 3: $Z_{avc}(z) = \dfrac{Z_e(z) Z_{e_avc}(z)}{Z_e(z) - Z_{e_avc}(z)}$ (5.14)

$$\text{Step 4: } k_{avc} = \left[\frac{-\mathrm{Im}(Z_{avc}(z))(\mathrm{Re}(s)^2 + \mathrm{Im}(s)^2)}{\mathrm{Im}(s)} \right]_{s \to \frac{T(z-1)}{2(z+1)}} \tag{5.15}$$

$$b_{avc} = \left[\mathrm{Re}(Z_{avc}(z)) - \frac{k_{avc}\,\mathrm{Re}(s)}{(\mathrm{Re}(s)^2 + \mathrm{Im}(s)^2)} \right]_{s \to \frac{T(z-1)}{2(z+1)}} \tag{5.16}$$

The parameters of adaptive virtual coupling, b_{avc} and k_{avc}, with respect to frequency are presented in chapter 6. The next section describes the implementation of the adaptive virtual coupling.

5.2 Implementation Procedure

In order to implement the adaptive virtual coupling, there are two components, i.e. the interacting frequency estimator and the adaptation procedure, added in the system as illustrated in figure 5.4. The parameters of the virtual coupling, i.e. b_{avc} and k_{avc}, are frequency dependent. Therefore, the frequency, which represents the response of human perceived impedance of haptic system with adaptive virtual coupling ($Z_{h_avc}(z)$), has to be determined in order to be used for adjusting the parameters of the virtual coupling. This frequency, which is called interacting frequency (IF) could be a point or a range of frequency characterized by haptic interaction.

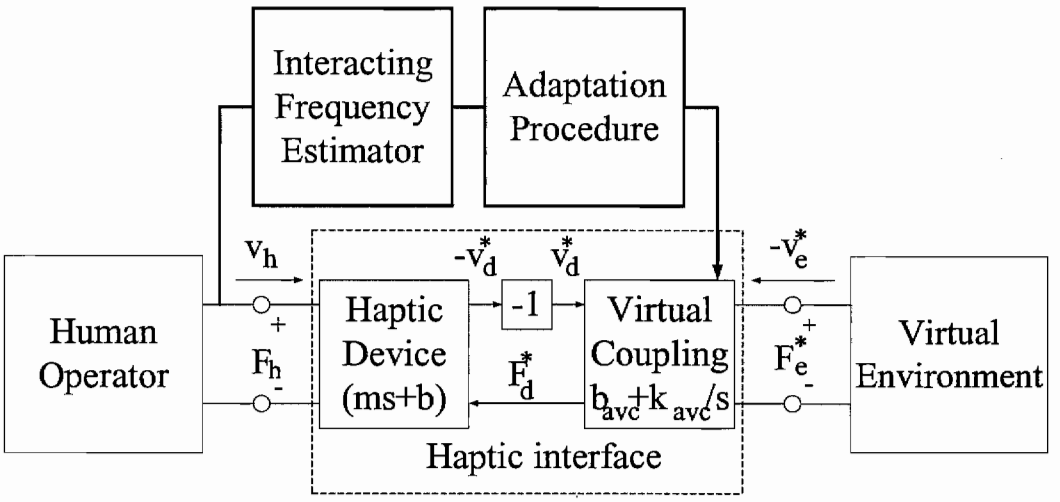

Figure 5.4 Schematic Diagram of a Haptic System with an Adaptive Virtual Coupling

These components are used for adjusting the parameters of the virtual coupling. From the outset of our derivation we assumed that all our system, i.e. human, haptic device and virtual environment, are LTI (Linear Time Invariant) systems as shown in figure 5.5.

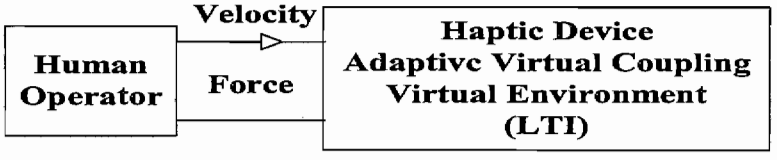

Figure 5.5 Schematic Diagram Shows that the Haptic System is a LTI System

Thus, the difference between input (velocity) and output (force) of the system should be only in magnitude and phase but have the same frequency. For this reason,

the interacting frequency could be directly determined from the spectral density of the velocity (S_v) of haptic interaction as.

$$S_v = \mathrm{FFT}(v_h), \tag{5.17}$$

where v_h is interacting velocity captured from haptic device. The interacting frequency could be determined at the peak frequency as shown in figure 5.6.

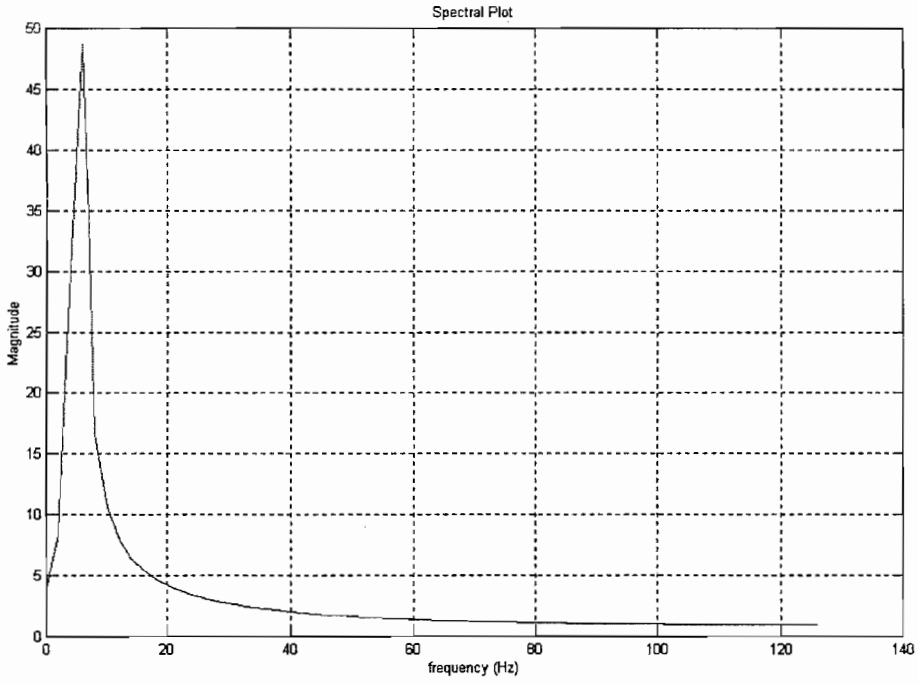

Figure 5.6 Spectral Density of the Velocity of a Haptic Interaction

Another parameter that should be concerned is the number of sampling of velocity data used for finding spectral density. Based on Burdea [12], frequency range that human can comfortably actuate is between 5 to 10 Hz. Thus, the number

of data that is sufficient for determining human interacting frequency should be about 20 samples. However, the number of sampled data we used are 128 samples, because this number of sampled data is the maximum data that the interacting frequency estimated routine can implement in updating rate of 1KHz.

The next chapter shows the experimental results which are the results of finding the realistic performance boundaries and the results on evaluation of adaptive virtual coupling.

Chapter 6

Experimental Results and Discussions

There are two experiments in this research, which are the experiment for determining the realistic performance boundaries and the experiment for evaluating on the realistic performance of the adaptive virtual couplings. In our experiment, ten subjects participated using the High Bandwidth Force Display with one degree of freedom (1-DOF) virtual environment. Six cases of referenced virtual environment impedance were used varied from nearly free motion impedance to constraint impedance. These referenced virtual environment impedance comprised of very low impedance (VE1) is the case that b_e and k_e are 10 N.s/m and 10 N/m respectively; low impedance (VE2) is the case that b_e and k_e are 10 N.s/m and 1000 N/m respectively; medium impedance (VE3) is the case that b_e and k_e are 10 N.s/m and 10000 N/m respectively; high impedance (VE4) is the case that b_e and k_e are 10 N.s/m and 25000 N/m respectively; very high impedance (VE5) is the case that b_e and k_e are 10 N.s/m and 50000 N/m respectively and constraint impedance (VE6) is the case that b_e and k_e are 10 N.s/m and 100000 N/m respectively.

The first section describes the experimental results and discussions on the determination of the realistic performance boundaries for these virtual environments. These realistic performance boundaries will be used as the performance index in formulating the parameters of the adaptive virtual coupling in the second section.

The third section describes the implementation and evaluation of the adaptive virtual coupling.

6.1 Experiment I: Determination of the Realistic Performance Boundaries

The objective of this experiment is to find the parameters of the realistic performance boundaries of these virtual environments. Our virtual environment was a virtual wall as shown by a dotted line in figure 6.1.

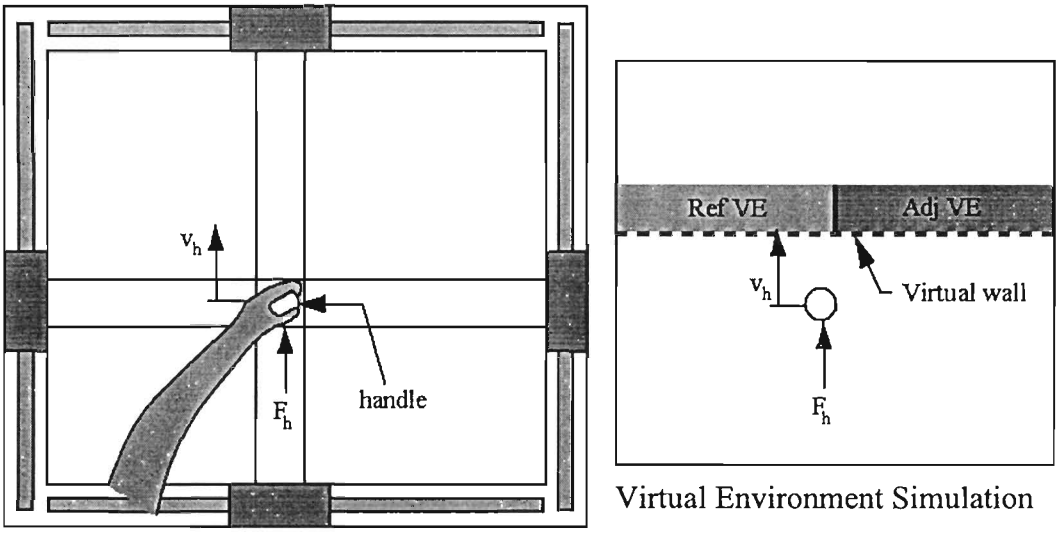

Figure 6.1 Virtual Wall Simulation. (Note that Ref VE and Adj VE are Referenced and Adjustable Virtual Environment Respectively)

As shown in figure 6.1, the adjustable virtual environment is placed beside the referenced virtual environment in order to compare the force feedback between these two environments. The updated force, corresponding to the adjusted parameters, is displayed in real-time. Therefore, users can perceive the updated

forces while adjusting the parameters. Users can also adjust parameters of the virtual environment (b_{e_adj}, k_{e_adj}) until he or she feels like interacting with the reference virtual environment. The final adjusted parameters were analyzed by using the confidence interval theory among all subjects and shown in Table.1.

Table 6.1 Experimental Results on the Determination of the Realistic Performance Boundaries (Note that VE is Virtual Environment, Stiffness is in N/m and Damping is in N.s/m)

VE	Parameters	Ref VE	LCI	UCI
VE 1	k_e	10	10.808	19.02
	b_e	10	7.895	12.265
VE 2	k_e	1000	944.85	1017.2
	b_e	10	8.404	12.316
VE 3	k_e	10000	8979.9	9954.1
	b_e	10	8.188	13.146
VE 4	k_e	25000	23316	24968
	b_e	10	8.447	12.549
VE 5	k_e	50000	39498	47829
	b_e	10	7.933	12.345
VE 6	k_e	100000	76795	62414
	b_e	10	6.328	15.863

From Table 6.1, the lower and upper bounds of parameters for each virtual environment are calculated. Such that the realistic performance boundaries of each referenced virtual environment, which are VE1, VE2, VE3, VE4, VE5 and VE6, are found and plotted in figure 6.2.

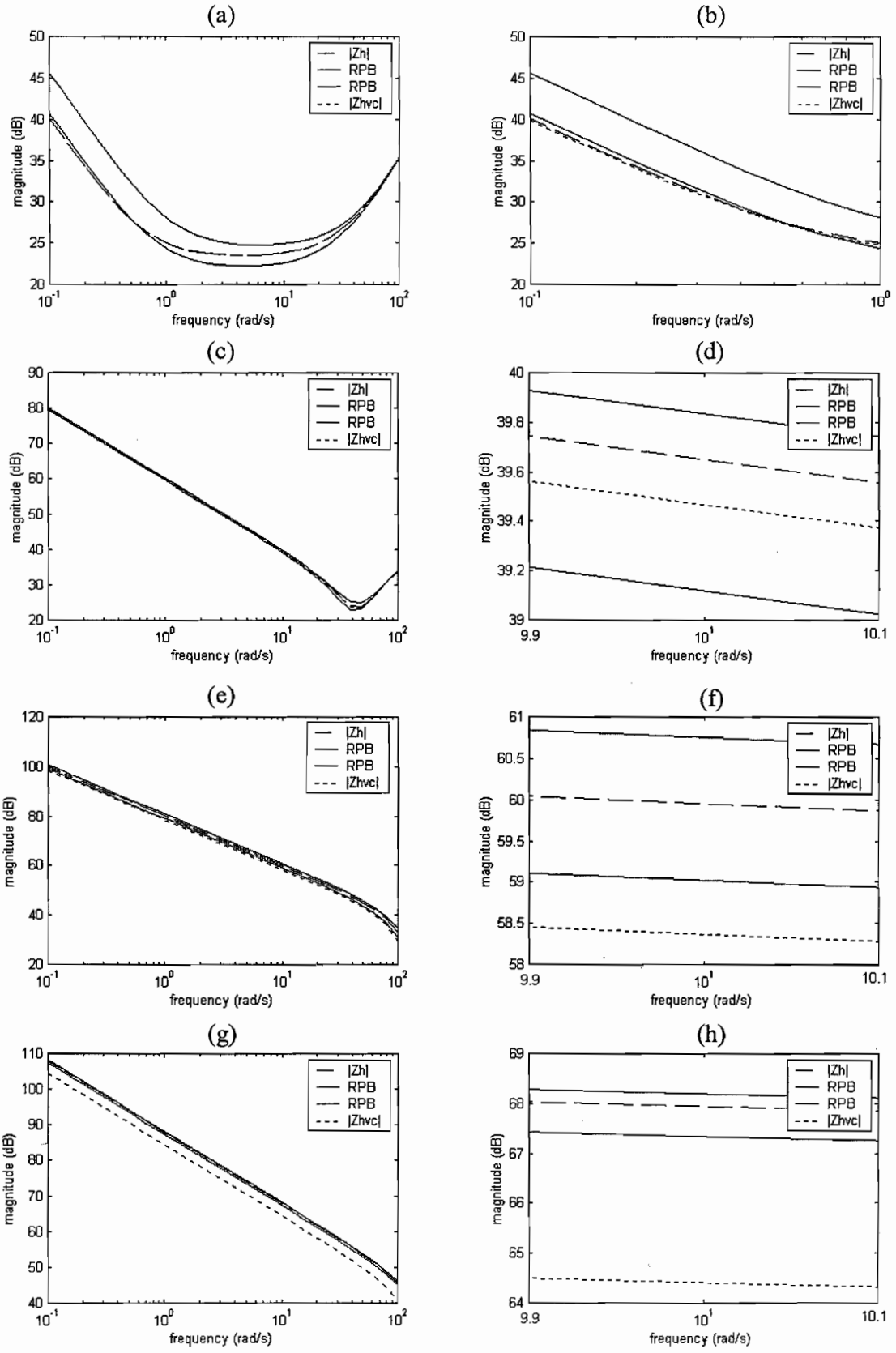

Figure 6.2 Plot of Realistic Performance Boundaries (Solid-Line)

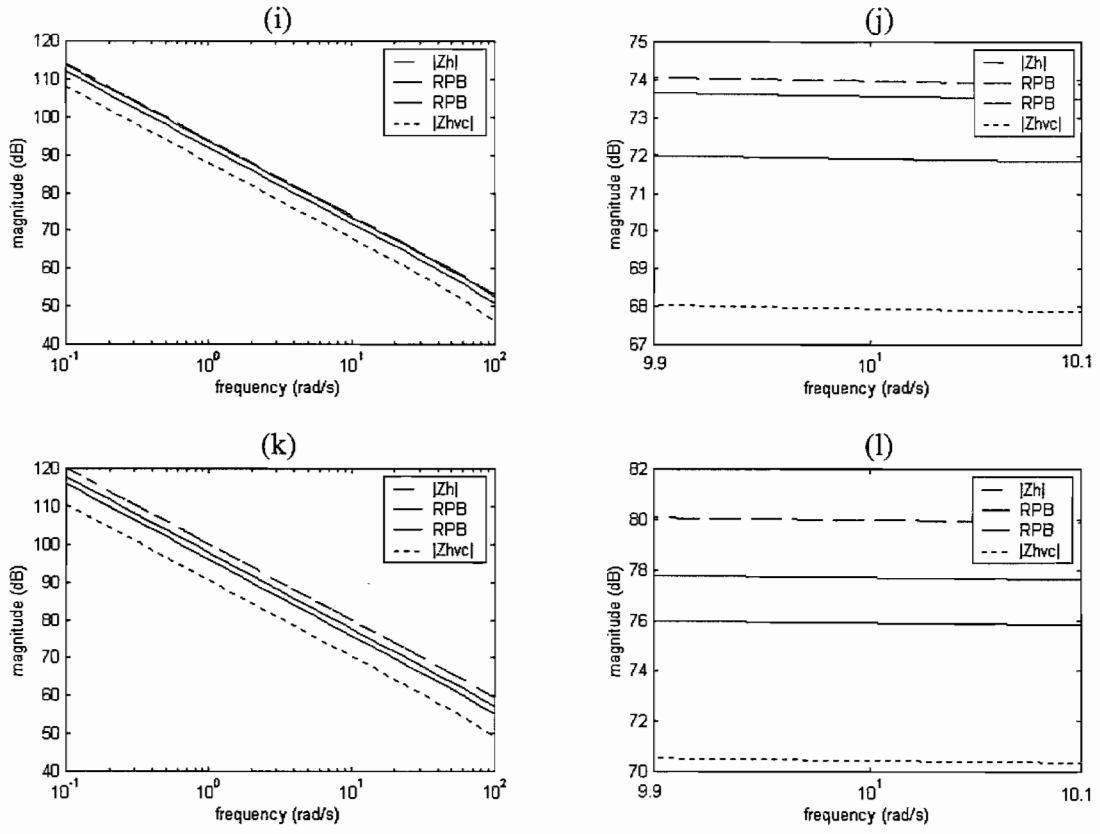

Figure 6.2 Plot of Realistic Performance Boundaries (Solid-Line) (Continued) $Z_h(z)$ (Long-Dash-Line) and $Z_{h_vc}(z)$ (Short-Dash-Line) when the Damping of the Virtual Environment is b_e = 10 N.s/m and the Stiffness are (a) VE1: k_e = 10 N/m, (b) Enlarged Figure of Figure 6.2a, (c) VE2: k_e = 1000 N/m, (d) Enlarged Figure of Figure 6.2c, (e) VE3: k_e = 10000 N/m, (f) Enlarged Figure of Figure 6.2e, (g) VE4: k_e = 25000 N/m, (h) Enlarged Figure of Figure 6.2g, (i) VE5: k_e = 50000 N/m, (j) Enlarged Figure of Figure 6.2i, (k) VE6: k_e = 100000 N/m, (l) Enlarged Figure of Figure 6.2k.

The short-dash-line is a plot of human perceived impedance of a haptic interface with a static virtual coupling ($Z_{h_vc}(z)$). The long dash-line is a plot of human perceived impedance of a haptic interface without virtual coupling ($Z_h(z)$) while the solid-lines are upper and lower boundaries. As shown in Fig. 6.2a, 6.2c, 6.2e, 6.2g, 6.2i and 6.2k, these four lines could not be distinguished. Hence, we also plotted figure 6.2b as an enlarged figure of these four lines at frequency between 0.1 rad/s to 1 rad/s and figure 6.2d, 6.2f, 6.2h, 6.2j and 6.2l are enlarged figures of these four lines at frequency between 9.9 rad/s to 10.1rad/s.

From figure 6.2e, 6.2g, 6.2i and 6.2k, it can be seen that the plots of these three different virtual environments have similar shape but different magnitude. The magnitude is high when the virtual environment has high impedance and low when the virtual environment has low impedance. Apparently that at high frequency, the plot of VE1 and VE2, which are low impedance virtual environments, are different from the other environments. The increasing in the magnitude of the impedance of these two cases are affected by the mechanical impedance of the haptic device.

Figure 6.2b, plot of $Z_{h_vc}(z)$ is almost the same line as plot of $Z_h(z)$ but both of them lie below the realistic performance boundaries. Thus, we can conclude that at low impedance virtual environment the effect of virtual coupling on realistic performance is not significant. We also observed that boundaries of impedance which allow human to feel like interacting with the nearly-free motion impedance, are higher than the impedance that the haptic system can display. Therefore, there are minimum impedance boundaries that human can perceive called minimum free motion impedance boundaries. For these reasons, there is no need to adjust the

parameters of the virtual coupling. Hence, we will not analyze the parameters of the adaptive virtual coupling for case of such a virtual environment.

Figure 6.2d shows that both plots of $Z_{h_vc}(z)$ and $Z_h(z)$ are in the realistic performance boundaries. The plot of $Z_{h_vc}(z)$ lies below $Z_h(z)$. Thus, we can conclude that human perceived impedance is decreased from the effect of virtual coupling. However, $Z_{h_vc}(z)$ satisfies the realistic performance boundaries.

In figure 6.2f, 6.2h, 6.2j and 6.2l, plots of $Z_{h_vc}(z)$ and $Z_h(z)$ are outside the realistic performance boundaries. Thus, users would perceive unrealistic interaction. In figure 6.2j, 6.2l, plot of $Z_h(z)$ lies above the upper boundary, thus we can conclude that human perception in constraint motion has limitation. As the consequence of this limitation, we can display the realistic interaction of referenced virtual environment if the displayed impedance is within the realistic boundaries.

From figure 6.2b, 6.2d, 6.2f, 6.2h, 6.2j and 6.2l, the band of realistic performance boundaries is the difference between upper and lower boundaries of interaction. This band has some relationship with the virtual environment impedance. It is small when interacting with low impedance environment and large when interacting with high impedance environment. Based on this observation, we can conclude that at low impedance simulation, the ability of human perception to distinguish the difference in virtual environment impedance is higher than one at high impedance simulation.

The human perceived impedance, displayed from the haptic system with an impedance-type virtual coupling, is always smaller than the impedance of the virtual environment. Therefore, the static virtual coupling may affect the realistic

performance of the haptic system. The static virtual coupling parameters, which are derived for guaranteeing overall system stability, are only suitable for high impedance simulation. However, for the simulation with lower or medium impedance, the human perceived impedance with static virtual coupling may not be within the realistic performance boundaries. Thus, criteria for adjusting the virtual coupling impedance so that the human perceived impedance can satisfy both stability criteria and realistic performance boundaries, should be thoroughly investigated.

The next section describes the calculation of the parameters for the adaptive virtual couplings of these environments.

6.2 Calculation of the Parameters for the Adaptive Virtual Couplings

The previous section provides us the parameters of the realistic performance boundaries. Thus, by following the steps in section 5.1, the parameters of the adaptive virtual coupling with respect to frequency would be determined. Furthermore, in order to verify system stability, a very stiff virtual environment (VE7: $b_e = 10$ N.s/m, $k_e = 180000$ N/m) is used as a critical testing case. Due to the human perception limitation in constraint motion mentioned in the previous section, the parameters of the virtual coupling of VE7 are determined based on the realistic performance boundaries of VE6 (a constraint impedance virtual environment). The results, which are b_{avc}, k_{avc}, $|Z_h|$ and $\mathrm{Re}(Z_h)$, of VE2, VE3, VE4, VE5, VE6 and VE7 are illustrated in figure 6.3, figure 6.4, figure 6.5, figure 6.6, figure 6.7 and figure 6.8, respectively.

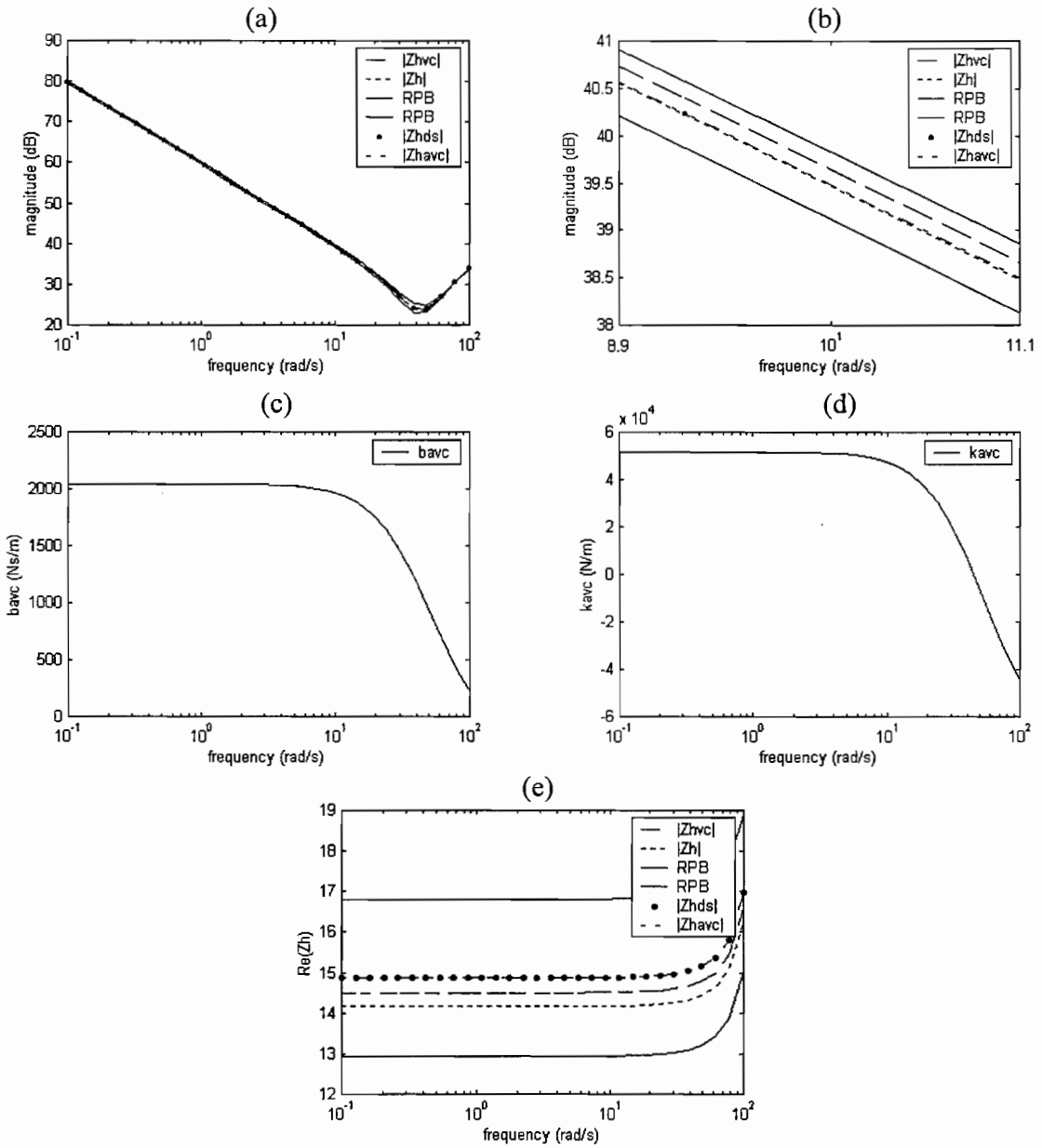

Figure 6.3 Plot of the Results on the Determination of the Adaptive Virtual Coupling of VE2 ($b_e = 10$ N.s/m, $k_e = 1000$ N/m)

(a) Plot of Human Perceived Impedance, (b) Enlarged Figure of Figure 6.3a, (c) Plot of b_{avc}, (d) Plot k_{avc} and (e) Plot of $Re(Z_h(z))$

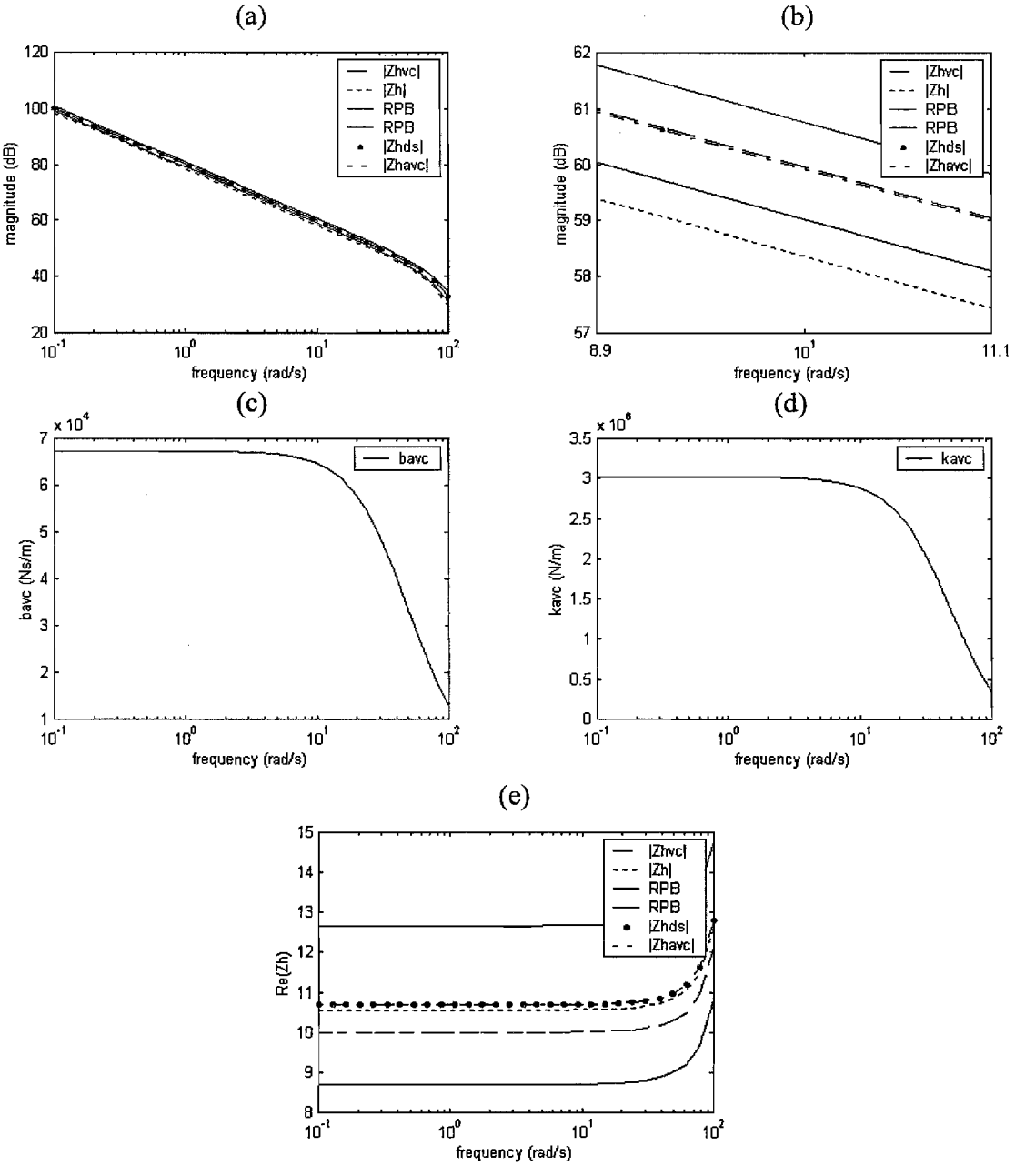

Figure 6.4 Plot of the Results on the Determination of the Adaptive Virtual Coupling of VE3 ($b_e = 10$ N.s/m, $k_e = 10000$ N/m)

(a) Plot of Human Perceived Impedance, (b) Enlarged Figure of Figure 6.4a, (c) Plot of b_{avc}, (d) Plot k_{avc} and (e) Plot of $Re(Z_h(z))$

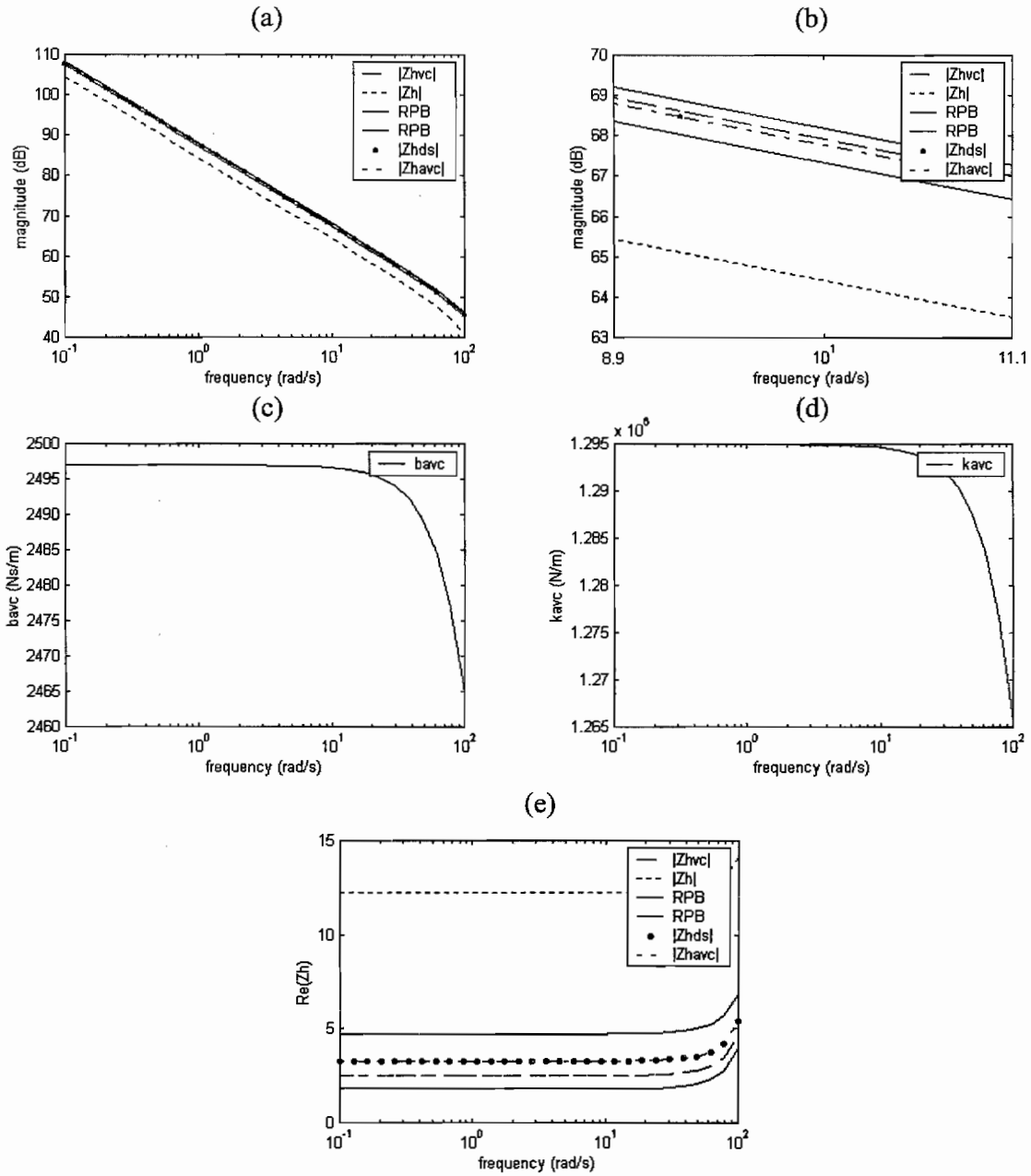

Figure 6.5 Plot of the Results on the Determination of the Adaptive Virtual Coupling of VE4 ($b_e = 10$ N.s/m, $k_e = 25000$ N/m)

(a) Plot of Human Perceived Impedance, (b) Enlarged Figure of Figure 6.5a, (c) Plot of b_{avc}, (d) Plot k_{avc} and (e) Plot of $Re(Z_h(z))$

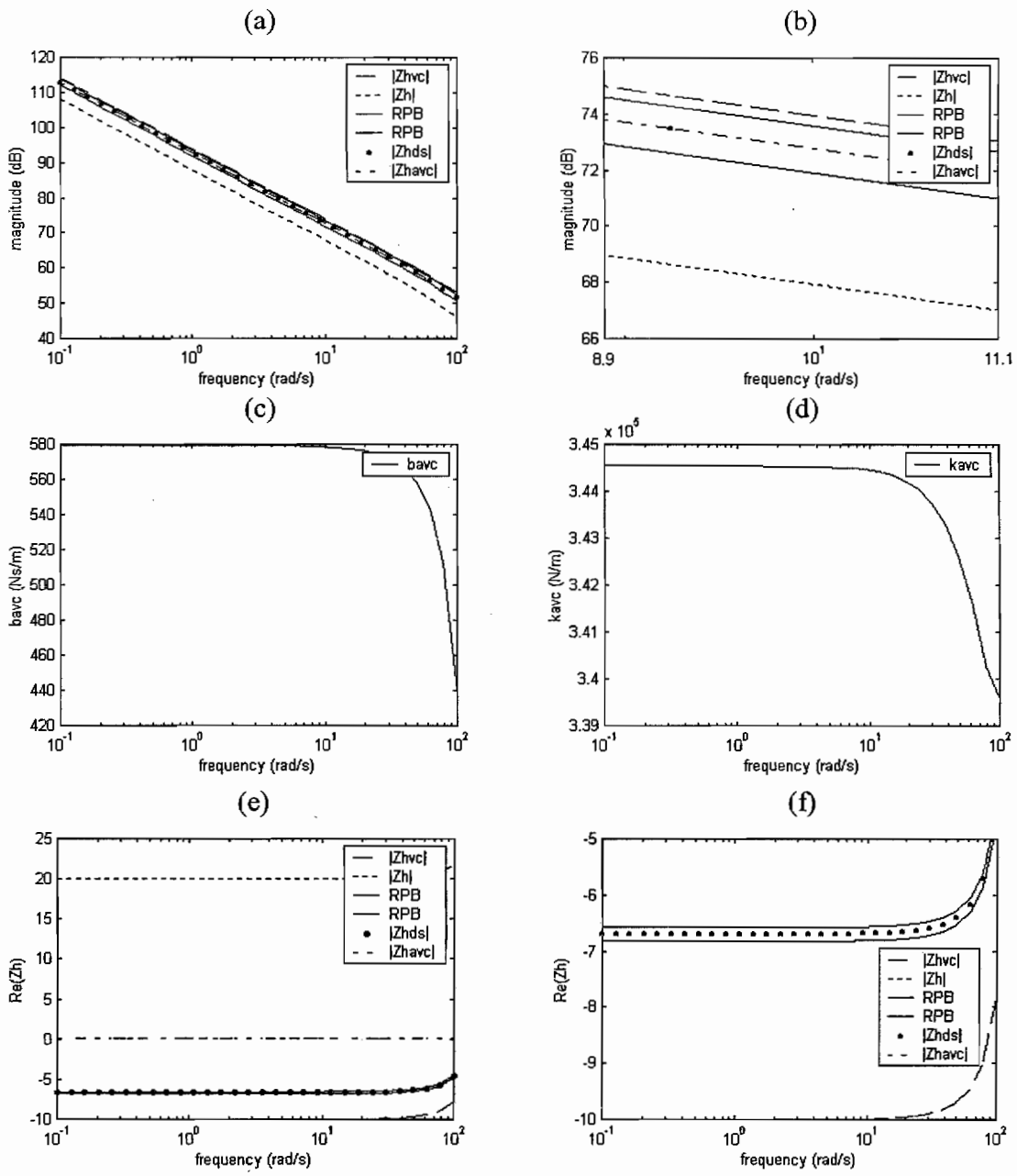

Figure 6.6 Plot of the Results on the Determination of the Adaptive Virtual Coupling of VE5 (b_e = 10 N.s/m, k_e = 50000 N/m)

(a) Plot of Human Perceived Impedance, (b) Enlarged Figure of Figure 6.6a, (c) Plot of b_{avc}, (d) Plot k_{avc}, (e) Plot of $Re(Z_h(z))$ and (f) Enlarged Figure of Figure 6.6e

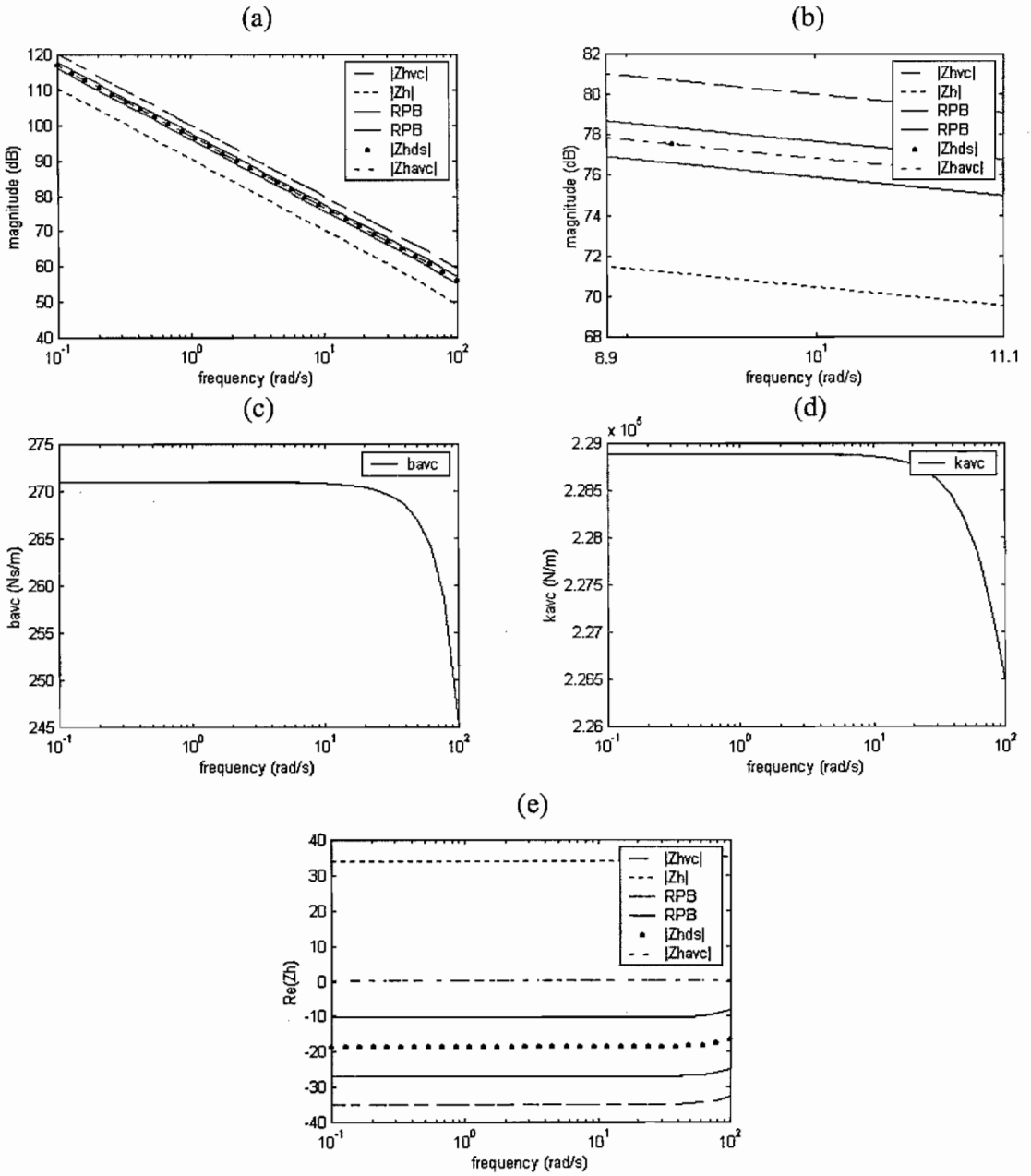

Figure 6.7 Plot of the Results on the Determination of the Adaptive Virtual Coupling of VE6 ($b_e = 10$ N.s/m, $k_e = 100000$ N/m)

(a) Plot of Human Perceived Impedance, (b) Enlarged Figure of Figure 6.7a, (c) Plot of b_{avc}, (d) Plot k_{avc} and (e) Plot of $Re(Z_h(z))$

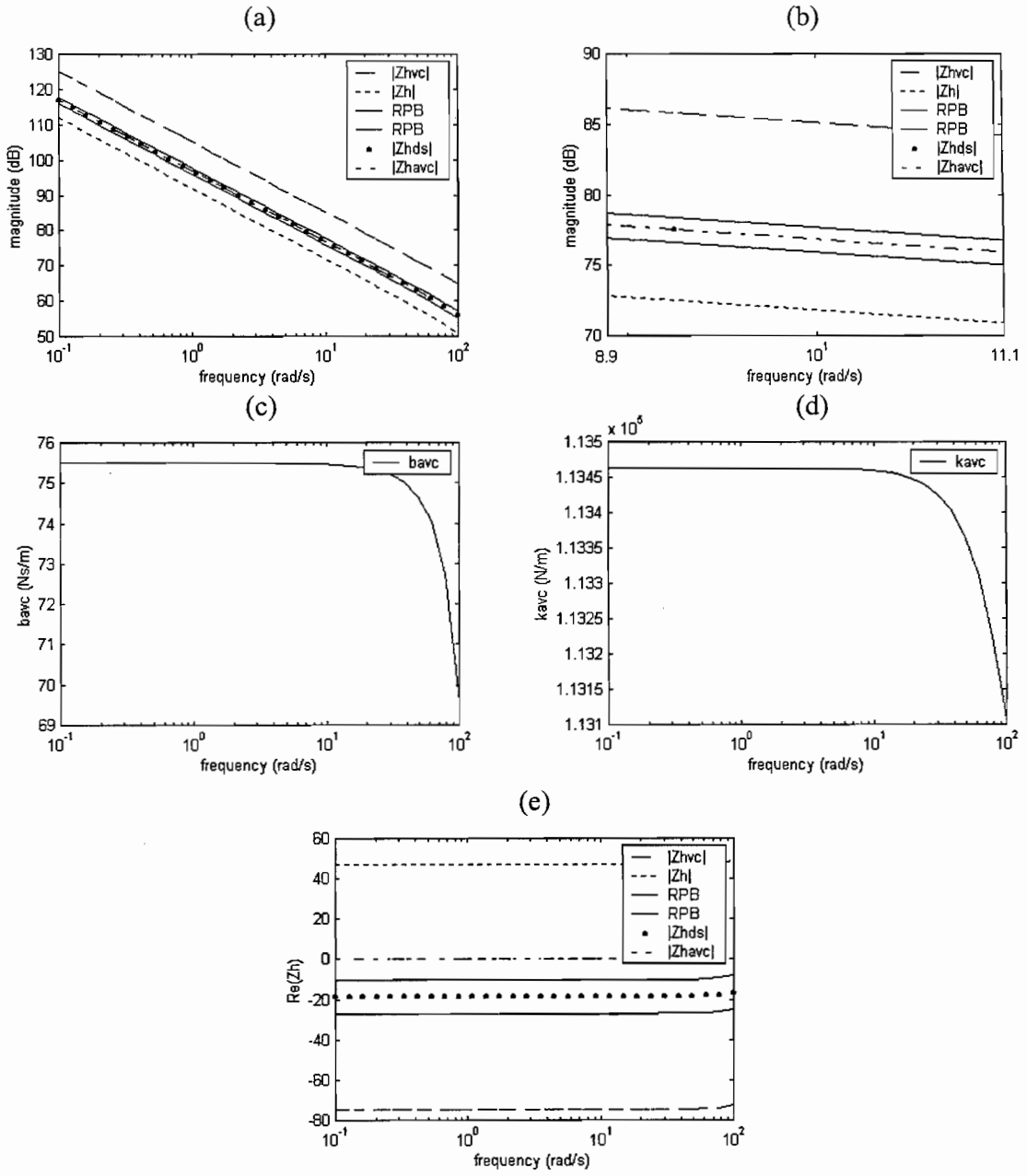

Figure 6.8 Plot of the Results on the Determination of the Adaptive Virtual Coupling of VE7 ($b_e = 10$ N.s/m, $k_e = 180000$ N/m)

(a) Plot of Human Perceived Impedance, (b) Enlarged Figure of Figure 6.8a, (c) Plot of b_{avc}, (d) Plot k_{avc} and (e) Plot of $Re(Z_h(z))$

The short-dash-line is a plot of human perceived impedance of a haptic interface with a static virtual coupling ($Z_{h_vc}(z)$). The long dash-line is a plot of human perceived impedance of a haptic interface without virtual coupling ($Z_h(z)$) while the solid-lines are upper and lower boundaries. The dash-dot-line is a plot of human perceived impedance of a haptic interface with adaptive virtual coupling ($Z_{h_avc}(z)$), while the dotted-line is the desired impedance. As shown in figure 6.3a, 6.4a, 6.5a, 6.6a, 6.7a and 6.8a, these four lines could not be distinguished. Hence, we also plotted figure 6.3b, 6.4b, 6.5b, 6.6b, 6.7b and 6.8b as enlarged figures of these four lines at frequency between 9.7 rad/s to 10.3 rad/s, 9 rad/s to 11 rad/s, 9.5 rad/s to 10.5 rad/s, 8 rad/s to 12 rad/s, 5 rad/s to 15 rad/s and 5 rad/s to 15 rad/s, respectively.

From these results, two criteria that we concerned are the stability and the realistic performance of the haptic system. The objectives of an adaptive virtual coupling are to eliminate or reduce the unrealistic of haptic interaction caused by the static virtual coupling while ensuring system stability. From figure 6.3e, 6.4e, 6.5e, 6.6e, 6.7e and 6.8e, plot of $\mathrm{Re}(Z_{h_avc}(z))$ (dash-dot-line) shows that this term is greater than zero, therefore the system satisfies the stability criteria in all cases of environments. From figure 6.3b, 6.4b, 6.5b, 6.6b, 6.7b and 6.8b, the plots of human perceived impedance of a haptic interface with adaptive virtual coupling ($Z_{h_avc}(z)$) are located in the realistic performance boundaries. Thus these systems are said to be realistic haptic systems based on the concept of the realistic performance boundaries.

Equation (5.15) and equation (5.16) show that b_{avc} is proportional to k_{avc}, therefore these parameters have the same shape but different in magnitude as shown in figure 6.3c, 6.3d, 6.4c, 6.4d, 6.5c, 6.5d, 6.6c, 6.6d, 6.7c, 6.7d, 6.8c and 6.8d. Moreover, the magnitude of these parameters depends on the difference between $Z_e(z)$ and $Z_{e_avc}(z)$ which in turn depends on the difference between $Z_{h_avc}(z)$ and $Z_h(z)$ as mentioned in equation (5.14). Thus b_{avc} and k_{avc} are high in case of the difference is small and in other hand b_{avc} and k_{avc} are low when the difference is high. For example, the difference between $Z_{h_vc}(z)$ and $Z_h(z)$ of VE3 shown in figure 6.4b is very low, therefore b_{avc} and k_{avc} is considerably high comparing with others virtual environments.

The cases that should be concerned are in VE6 and VE7 as shown in figure 6.7 and 6.8. These cases are high stiffness virtual environments, which cannot be implemented directly without virtual coupling. Therefore, the desired impedance of these two cases are the same. However, the impedance of VE7 is greater than of VE6. Hence the difference of $Z_e(z)$ and $Z_{e_avc}(z)$ of VE7 is greater than of VE6. Thus the magnitude of b_{avc} and k_{avc} of VE6 is greater than of VE7 even $Z_e(z)$ of VE7 is greater than of VE6. These results are shown in figure 6.7c, 6.7d, 6.8c and 6.8d. From this observation, b_{avc} and k_{avc} are inversely proportional to the impedance of the virtual environment when the impedance of the virtual environment is higher than the maximum constraint impedance boundaries.

From figure 6.6e, 6.7e and 6.8e, it can be seen that, in case of no virtual coupling, the real-part of the realistic performance boundaries are negative thus $\mathrm{Re}(Z_{h_ds}(z)) < 0$. As these consequences, from equation (5.11) the

$Re(Z_{h_avc}(z)) > 0$ must be set to be greater than zero in order to ensure system stability. Thus, the adaptive virtual coupling not only enhances realistic performance, as done in VE2, VE3 and VE4, but also improves system stability.

The next section is the results on the evaluation of the realistic performance of the adaptive virtual coupling.

6.3 Experiment II : Evaluating the Realistic Performance of Adaptive Virtual Couplings

The final step is to qualitatively evaluate the performance of the adaptive virtual coupling system in comparison to the static virtual coupling. Our virtual environment was a virtual wall as shown by a dotted line in figure 6.9.

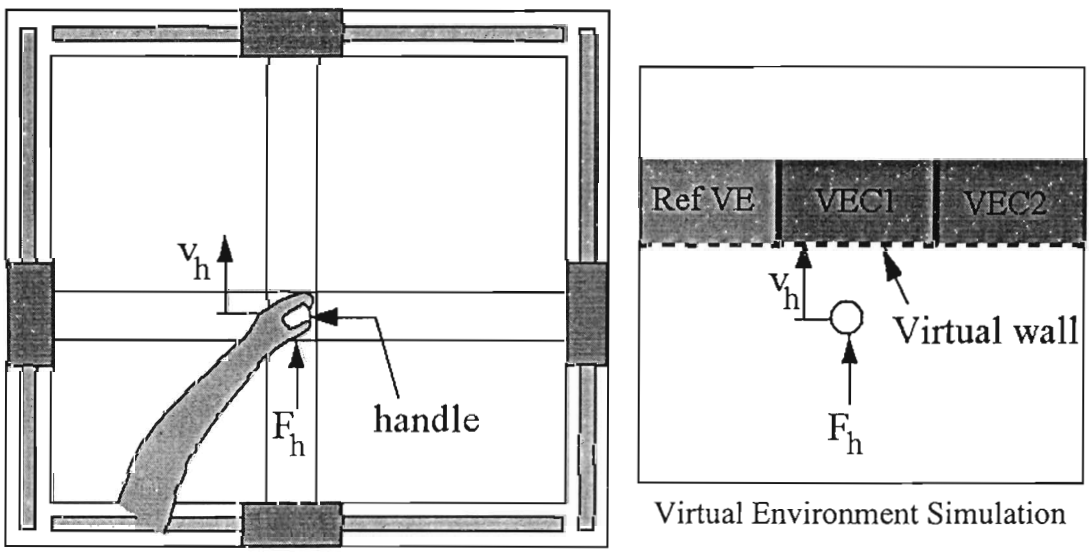

Figure 6.9 A Simulation Used as an Evaluation of Realistic Performance

(Note that: Ref VE, VEC1 and VEC2 are Referenced Virtual Environment, Referenced Virtual Environment with Virtual Coupling

(Number One) and Referenced Virtual Environment with Virtual Coupling (Number Two)

Based on the realism of interaction of each virtual environment, users were asked to match one of the simulations (VEC1 or VEC2) with the reference virtual environment (Ref VE). The VEC1 and VEC2 were randomly assigned to be the virtual environment with static virtual coupling or with adaptive virtual coupling. Such that, the user had no bias in the experiment. Moreover, the stability of the interactions was observed based on the convergence of the interaction velocity. The system is said to be a stable system if the velocity, eventually, converges to zero. The results are presented in the Table 6.2 and figure 6.10.

Table 6.2 Experimental Results on the Matching of the Virtual Environment

VEs	No VC	Static virtual coupling		Adaptive virtual coupling		Unable to match
	Stability	Stability	Realistic performance	Stability	Realistic performance	
	Stable	Stable	Matched with VE	Stable	Matched with VE	
VE 2	10	10	3	10	3	4
VE 3	10	10	3	10	5	2
VE 4	10	10	6	10	4	0
VE 5	4	10	1	10	9	0
VE 6	0	10	1	10	9	0
VE 7	0	10	2	10	8	0

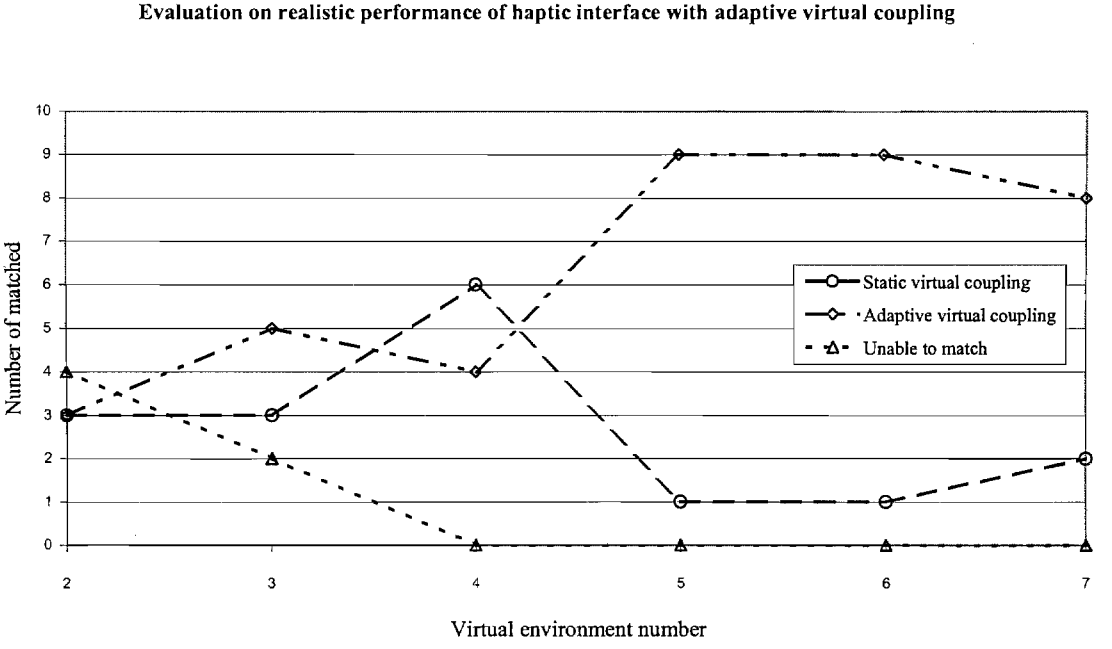

Figure 6.10 Plot of the Experimental Results on the Matching of the Virtual Environment

In the high stiffness virtual environments, such as VE5, VE6 and VE7, the realistic performance of the haptic system with adaptive virtual coupling is considerably increased as shown in figure 6.9. On the other hand, in the medium stiffness virtual environment, VE3 and VE4, user cannot distinguish the difference between two types of virtual coupling. Furthermore, in case of low stiffness: VE2, human could not even perceive the difference between the two simulations. These results show that the realistic performance of the haptic system with an adaptive virtual coupling is enhanced comparing with the haptic system with a static virtual coupling. However, the degree in improvement of the realistic performance depends on the impedance of the virtual environment. The adaptive virtual coupling enhances the realistic performance when it is used with the high stiffness virtual environment.

However, the adaptive virtual coupling does not increase the performance when it is used with very low impedance environment.

Chapter 7

Conclusions and Future Works

In this research, we proposed the realistic performance boundaries representing variation of human perceived impedance ($Z_h(z)$). These boundaries which depend on virtual environment impedance are delineated from the experimental data. Based on these boundaries, the realistic performance of the haptic system can be determined. We have found that the use of static virtual coupling in haptic systems could affect the realistic performance of the system. Therefore, an approach to enhance the realistic performance of haptic systems was proposed by adapting the parameters of the virtual coupling according to the virtual environment. A desired impedance is proposed in order to be used as our objective impedance. In Chapter 5, the method for determining the parameters of the virtual coupling with respect to frequency was proposed. Therefore, each defined virtual environment has its own set of parameters of virtual coupling that both ensure system stability and increase the realistic performance of system. These parameters are used as the adaptive parameters in the system in order to adjust the displayed impedance. Therefore, the displayed impedance approaches the desired impedance, which is derived from the realistic performance. Thus, the realistic performance is ensured. Moreover the stability is also guaranteed based on passivity theory. The evaluation of the realistic performance of the haptic system with adaptive virtual coupling was also

determined comparing to static virtual coupling. The results showed that the realistic performance of haptic system can be increased by using adaptive virtual coupling.

On a practical level, the contribution of this work is that all proposed concepts can be practically implemented and evaluated. We also developed a windows-based program for controlling our testbed at the updating rate of 1kHz.

From the discussion of the realistic performance boundaries, the band of realistic performance has some relationship with the virtual environment impedance. For the low impedance environment, the band is small. For the high impedance environment, the band is large. Based on this observation, this relationship would be determined in the future works. Therefore, the realistic performance boundaries would be directly determined instead of obtaining through experiment all cases of virtual environments.

This thesis is based on the known virtual environment. However, in actual implementation, the virtual environment model is unknown. Thus, an interesting future work is to find an algorithm used for determining a real-time virtual environment model.

Reference

1. Colgate, E. J., Stanley, M.C. and Brown, M.J., 1995, "Issues in the Haptic Display of Tool Use," **Proceedings of the 1995 IEEE/RSJ International Conference on Intelligent Robots and Systems**

2. Colgate, E.J. and Schenkel, G., 1994, "Passivity of a Class of Sampled-Data Systems: Application to Haptic Interfaces," **American Control Conference,** Baltimore

3. Adams, J. R. and Hannaford, B., 1998, "A Two-Port Framework for the Design of Unconditionally Stable Haptic Interfaces," **Proceedings of the 1998 IEEE/RSJ International Conference on Intelligent Robots and Systems**, pp. 1254-1259.

4. Adams, J.R., Moreyra, M.R. and Hannaford, B., 1998, "Stability and Performance of Haptic Displays: Theory and Experiments," **Proceedings of ASME International Mechanical Engineering Congress and Exhibition,** Anaheim California, pp. 227 - 234.

5. Adams, J.R., and Hannaford, B., 1999, "Control Law Design for Haptic Interfaces to Virtual Reality," **IEEE Transactions on Control System Technology.**

6. Adams, J. R. and Hannaford, B., 1999, "Stable Haptic Interaction with Virtual Environments," **IEEE Transactions on Robotics and Automation**, June, Vol. 15, No. 3

7. Ryu, H. J. and Hannaford, B., 2001, "Time Domain Passivity Control of Haptic Interfaces," **Proceeding of the 2001 IEEE International Conference on Robotics and Automation**, Vol. 2, pp. 1863 –1869.

8. Colgate, E. J. and Brown, M.J., 1994, "Factors Affecting the Z-Width of a Haptic Display," **Proceeding of IEEE International Conference on Robotics and Automation**, Los Alamitos, pp. 3205-3210.

9. Lawrence A.D. and Chapel, D.J., 1994, "Performance Trade-Offs for Hand Controller Design," **IEEE of International Conference on Robotics and Automation**, pp. 3211-3216.

10. Yokokohji, Y., Hollis, R. and Kanade, T., 1996, "What You Can See is What You Can Feel," **IEEE Virtual Reality Annual International Symposium,** Santa Clara California.

11. Moreyra, M. and Hannaford, B., 1998, "A Practical Measure of Dynamic Response of Haptic Devices," **Proceedings of the 1998 IEEE International Conference on Robotics and Automation**, Belgium

12. Burdea, C.G., 1996, Force and Touch Feedback for Virtual Reality, A Wiley-Interscience-Publication, pp. 71-74.

13. Kuh, S.E. and Rohrer, A.R., 1967, Theory of Linear Active Networks, Berkeley, Holden-Day, pp. 115-166.

14. Hogan, N., 1989, "Controlling Impedance at the Man/Machine," **Proceeding of the 1989 IEEE International Conference on Robotics and Automation**, pp. 1626-1631.

15. Moreyra, M. and Hannaford, B., 1996, Design of a planar High Bandwidth Force Display with Force Sensing, Master of Science in Electrical Engineering Thesis, Electrical Engineering Program, University of Washington

16. Brown, M.J., 1998, Passive Implementation of Multibody Simulations for Haptic Display, Doctor of Philosophy Dissertation, Mechanical Engineering Program, Northwestern University

17. Lertpolpairoj, S., Maneewarn, T., Charoenseang, S. and Laowattana, D. 2001, "The Effect of Static Virtual Couplings on Realistic Performance of Haptic Systems," **The 4th Asian Conference on Robotics and Its Applications**, 6 June 2001, Singapore, pp. 57-63

มหาวิทยาลัยเทคโนโลยีพระจอมเกล้าธนบุรี
ข้อตกลงว่าด้วยการโอนลิขสิทธิ์วิทยานิพนธ์

วันที่ 20 เดือน พฤศจิกายน พ.ศ. 2544

ข้าพเจ้า นาย สมพงศ์ เลิศผลไพโรจน์ รหัสประจำตัว 41400146 เป็นนักศึกษาของมหาวิทยาลัยเทคโนโลยีพระจอมเกล้าธนบุรี ระดับปริญญา ☑ โท ☐ เอก
หลักสูตร ปริญญาวิศวกรรมศาสตรมหาบัณฑิต สาขาวิชา เครื่องกล คณะ วิศวกรรมศาสตร์
อยู่บ้านเลขที่ 125/61 ม.3 ตรอก/ซอย เอกชัย36 ถนน เอกชัย
ตำบล/แขวง บางขุนเทียน อำเภอ/เขต จอมทอง จังหวัด กรุงเทพฯ
ระหัสไปรษณีย์ 10150 ขอโอนลิขสิทธิ์วิทยานิพนธ์ให้ไว้กับ มหาวิทยาลัยเทคโนโลยีพระจอมเกล้าธนบุรี โดยมี รศ.เกษม เพชรเกตุ ตำแหน่ง คณบดีวิศวกรรมศาสตร์ เป็นผู้รับโอนลิขสิทธิ์และมีข้อตกลงดังนี้

1. ข้าพเจ้าได้จัดทำวิทยานิพนธ์เรื่อง An Improvement of Realistic Performance of a Haptic System with an Adaptive Virtual Coupling ซึ่งอยู่ในความควบคุมของ ดร. สยาม เจริญเสียง ตามมาตรา 14 แห่ง พ.ร.บ. ลิขสิทธิ์ พ.ศ. 2537 และถือว่าเป็นส่วยหนึ่งของการศึกษาตามหลักสูตรของมหาวิทยาลัยเทคโนโลยีพระจอมเกล้าธนบุรี

2. ข้าพเจ้าตกลงโอนลิขสิทธิ์จากผลงานทั้งหมดที่เกิดขึ้นจากการสร้างสรรค์ของข้าพเจ้าในวิทยานิพนธ์ให้กับมหาวิทยาลัยเทคโนโลยีพระจอมเกล้าธนบุรี ตลอดอายุแห่งการควบคุมครองลิขสิทธิ์ตามมาตรา 23 แห่งพระราชบัญญัติลิขสิทธิ์ พ.ศ. 2537 ตั้งแต่วันที่ได้รับอนุมัติโครงร่างวิทยานิพนธ์จากมหาวิทยาลัย

3. ในกรณีที่ข้าพเจ้าประสงค์จะนำวิทยานิพนธ์ไปใช้ในการเผยแพร่ในสื่อใดๆ ก็ตาม ข้าพเจ้าจะต้องระบุว่าวิทยานิพนธ์เป็นผลงานของมหาวิทยาลัยเทคโนโลยีพระจอมเกล้าธนบุรีทุกๆครั้งที่มีการเผยแพร่

4. ในกรณีที่ข้าพเจ้าประสงค์จะนำวิทยานิพนธ์ไปใช้ในการเผยแพร่ หรืออนุญาตให้ผู้อื่นๆ ทำซ้ำหรือดัดแปลงหรือเผยแพร่ต่อสาธารณะชนหรือกระทำการใดๆ ตามมาตรา 27, มาตรา 28, มาตรา 29 และ มาตรา 30 แห่งพระราชบัญญัติลิขสิทธิ์ พ.ศ. 2537 โดยมีค่าตอบแทนทางธุระกิจ ข้าพเจ้าพร้อมจะกระทำได้โดยได้รับความยินยอมเป็นลายลักษณ์อักษรจากมหาวิทยาลัยเทคโนโลยีพระจอมเกล้าธนบุรี

ลงชื่อ ..... ผู้โอนลิขสิทธิ์
(สมพงศ์ เลิศผลไพโรจน์)

ลงชื่อ ..... ผู้รับโอนลิขสิทธิ์
(รศ. เกษม เพชรเกตุ)

ลงชื่อ ..... พยาน
(ดร. สยาม เจริญเสียง)

ลงชื่อ ..... พยาน
(ผศ. ดร. พิชิต ฤกษนันทน์)